SIMPLIFIED PLASTIC LIMIT ANALYSIS OF DRAG EMBEDMENT ANCHORS IN LAYERED COHESIVE SOILS

A Thesis

by

MARCUS P. RASULO

Submitted to the Office of Graduate and Professional Studies of
Texas A&M University
in partial fulfillment of the requirements for the degree of

MASTER OF SCIENCE

Chair of Committee,	Charles Aubeny
Committee Members,	Marcelo Sanchez
	Jerome Schubert
Head of Department,	Robin Autenrieth

May 2016

Major Subject: Civil Engineering

ABSTRACT

Drag embedment anchors (DEA) are widely used for the temporary, and to a lesser extent the permanent mooring of offshore structures. While they can provide an effective mooring solution, the most commonly used design method, the empirical design charts, leave a high level of uncertainty in prediction of the capacity and trajectory of installed anchors. While this is partially alleviated through the standard of proof loading installed anchors, improved models are needed to help predict the complete capacity and trajectory of the anchors. The presence of layered soils presents an especially complex challenge, which is beyond the scope of most current models. Instead, designers must rely on past experience in the region and designer judgment to estimate if the anchor will be able to penetrate through these challenging soils.

Plastic limit analysis (PLA) allow the incorporation of analytical solutions and geotechnical principles into the design of DEA. In PLA models, the behavior of the anchor is governed by a yield locus, which combined with an incremental kinematic model it can be used to estimate the capacity and movement of the anchor as it advanced through the soil.

The model proposed here is a simplified PLA that assumes a steady state condition as the anchor is embedded. In this state, the anchor load angle or padeye angle is assumed to align with the anchors fluke-shank angle resulting in a condition of zero moment and simplified rotational behavior. The model is then compared to a series of existing design charts, and results from full-scale field installations. To address the issue

of layered soils the framework of the model is then expanded to allow for the inclusion of stiff layers of clays. The stiff layers are analyzed through the use of area transformations and multipliers equivalent to the area of the anchor embedded into the layer. As no non-proprietary data is available to validate the model at this time, the model is then simulated through a number complex configurations to see how it captures known behavior.

ACKNOWLEDGEMENTS

While the completion of this achievement marks a major achievement in my life none of it would have been possible without the people who supported me in reaching this point. I would like to thank my advisor, Dr. Charles Aubeny, who has guided me through my research. His patience and the depth of his technical knowledge set standards I will strive to reach throughout my career.

I would like to thank my committee, Dr. Marcelo Sanchez, and Dr. Jerome Schubert for the support and input. Through this research and the time Dr. Sanchez spent advising me in the Geo-Institute both have shown me the duty we owe to our profession as a community.

I would like to thank my parent, who instilled in me curiosity that has led me to this point and equipped me with the perseverance to never give in.

I would like to thank my friends who have commiserated with me throughout the challenges and joys of graduate school. Especially Jeff Miles, who has served as a mentor, and embodied the spirit of Texas A&M University.

TABLE OF CONTENTS

Page

LIST OF FIGURES

Page

LIST OF TABLES

Page

1. INTRODUCTION

1.1 Overview

The challenges faced in offshore foundations create the need for a wide range of solutions. As with any engineering project selection of the most appropriate solutions combines balancing technically sound design to meet environmental conditions ensuring reliability, with economic feasibility.

As projects have pushed into more and more challenging conditions, new constraints have created drastic changes in how engineers design foundations. In the case of floating structures, where it is no longer practical to extend foundations directly to the seabed, the foundation consists of a mooring system, made up of mooring lines, and anchors. Floating structures may be employed for a variety of reasons ranging from projects in large water depths such as the Independence Hub in 8,000 ft (FMC Technologies, nd). of water, to temporary moorings for mobile offshore drilling units (MODU), or the future prospect of offshore floating wind and wave energy farms. With the large range in offshore structures there is also a wide range in anchoring systems. Concepts have been developed similar to onshore solutions such as driven piles as well as solution unique to offshore such as drag embedment anchors (DEA), suction caissons, and many others.

Drag embedment anchors (DEA) have proven to be an economical and practical solution to the needs of many projects. While DEA's have been widely and successfully installed around the world, the design of the anchors in practice has relied on heavily on the use of empirical design charts. These employ few site specific variables and instead

rely on broad soil characterization providing only the absolute minimum analysis required for the installation of DEA. The presence of layered soils creates an especially complex challenge as it is largely left up to the designer's judgment and past experience to estimate if the anchors will penetrate through the interfaces between layers. While these uncertainties are partially remedied through proof loads to test capacity during installation improved techniques are needed for prediction of capacity and trajectory as the anchors are installed.

The move to a more analytical framework began with the development of limit equilibrium models for clays and sands (Stewart 1992, and Neubecker and Randolph 1996, and Dahlberg 1998), and their adaptation for layered soils (O'Neil 2000). In an attempt to further reduce the empirical aspects of the design plastic limit analyses (PLA) models were developed for soft cohesive soils (O'Neill et al., 2003, Murff et al., 2005, Aubeny and Chi 2010). These analytical solutions presented a significant step forward allowing for the inclusion of site specific soil parameters, and complete trajectory and capacity histories of the anchor as it embeds.

The goal of this work is to provide a simplified PLA the methods for predicting the capacity and trajectory of DEA. The model will then be validated against field tests, and design charts. A proposed expansion to the model to accommodation the inclusion of stiff clay layers will then be presented and compared to expected behavior.

1.2 Drag Embedment Anchors

Drag embedment anchors (DEA) are plate anchors composed of a fluke, shank, and a padeye that are embedded by an anchor handling vessel (AHV) dragging them along the seabed. The anchor may initially drag along the surface until it sets in and begins to dive through the soil. Under ideal conditions the anchor will embed into the bed along a curved trajectory, with the fluke rotating from a steep angle to a horizontal one as it approaches its ultimate capacity, as shown in Figure 1. In soft cohesive soils the anchor acts like a deeply embedded plate mobilizing its resistance through the soil's shear strength and along the embedded portion of the mooring line. As shear strength typically increases with depth, the capacity of the anchor results from a combination of the penetration to stronger soils as well as maximizing the bearing area of the fluke.

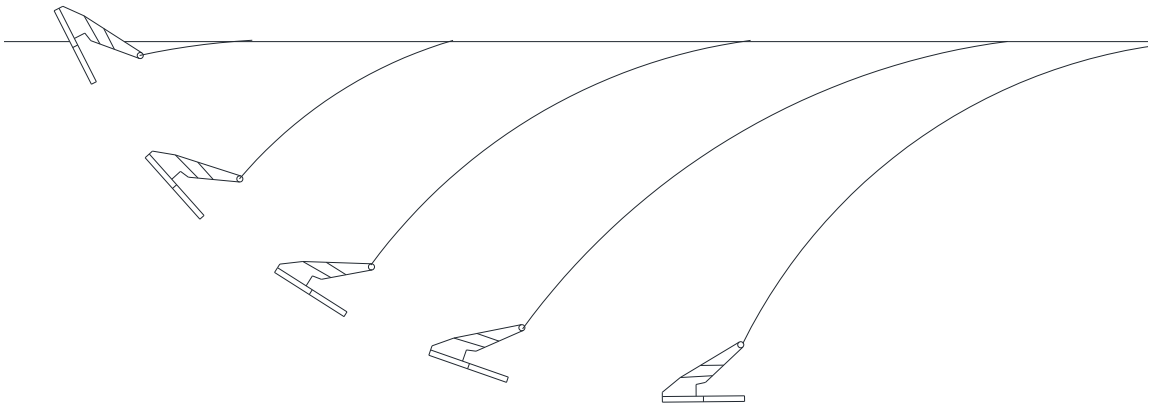

Figure 1: Anchor Embedment

DEAs are designed to resist in plane horizontal loads and are usually used as part of catenary mooring systems. In a catenary system mooring lines are configured extend from the structure to the seabed in a catenary configuration until it rests on the seabed at a horizontal angle resulting in primarily horizontal forces. If significant vertical forces may occur, as in a semi-taut mooring system is required a vertically loaded anchor (VLA) may be more suitable. VLAs are a modified version of DEA to allow them to provide vertical components of resistance. The sensitivity to out of plane loading does provide benefit ,as it allows the anchors to be retrieved using forces significantly below the loading capacity provided in plane.

Good anchor design typically involves minimizing the resistance tangential to the anchor to maximize embedment while maximizing the bearing area to maximize the pullout resistance. Additional fins and stabilizers are designed to reduce out of plane motion, roll and yaw of the anchor as it embeds. This typically results in an anchor with a double tooth in the direction of embedment.

DEAs can be configured for different soil conditions by adjusting the angle at which the shank connects to the fluke, called the fluke-shank angle, θ_{fs}. This can often be easily done offshore by removing a pin and adjusting the shank around a swivel. In clays where deep embedment can be expected, the θ_{fs} is typically set to approximately 50 degrees to maximize embedment. In stiff soils and sands it is typically set to approximate 30 degrees to balance achieving set-in and penetration. Anchors set at 50 degrees in stiff soil will tend to set in and trip along the seabed. While larger θ_{fs} typically result in high capacities, this must be balanced against ensuring the anchor will

embed into the soil. In addition to these two setting some anchors have intermediate settings for intermediate and more complex soils.

DEA provide an appealing solution due to their high efficiency (ratio of holding capacity to weight), ability to be retrieved and re-used, feasibility in deep water, and cost savings during installation. While the cost of manufacturing a DEA typically exceeds that of a pile, the overall costs can be lower due to decreased installation, and mobilization costs and time (Vryhoff, 2010). DEAs have been readily adopted for use in temporary moorings but are not as widely used in permanent moorings due to uncertainty in their capacity and location, due to the difficulty in predicting their embedment trajectory. While this uncertainty exists in the prediction, it is mitigated by the testing of proof loads in the field during installation.

If deep embedment can be expected and vertical components of load or taut moorings are required, the use of a VLA is recommended. VLAs are a form of DEA that have been adapted to resist vertical loads. They are installed in two stages, the first being identical to that of a DEA, and the second involving free shank loading. In the first stage of installation the VLA is embedded with a fixed shank until it reaches a desired drag distance or capacity as defined by the project. Installation techniques for VLAs vary according to the manufacturer. By one me the angle of the anchor line at the seabed is then increased to around 40 degrees and suddenly jerked to break a shear pin located in the anchor. Once sheared the shank is released to rotate freely. In free rotation the shank will seek a new geometric equilibrium and result in a higher θ_{fs} allowing the anchor to be loaded more normal to the fluke and therefore a higher capacity.

1.3 Layered Soils

Layered soils present a complex condition that most design methods do not directly address, but instead defer to designer judgment and past experience to estimate if they will penetrate the layer. In some cases of soft soils overlying stiff soils the anchors will be unable to penetrate into the stiff and trip along the interface between the two layers. This can result in a failure to reach the design capacity of the anchor. In other instances, the anchor can become partially embedded into the stiff layer and reach design capacities. This case can still provide a potential hazard as the anchor will fail to reach the expected penetration and be highly sensitive to loading out of the plane of the shank and vertical loading. While typically designed to avoid out of plane loading, it may be experienced due to unanticipated conditionals or in the case of an accidental limit state condition where other mooring lines have failed.

1.4 Objective of Research

Drag embedment anchors provide a practical solution for the mooring of floating offshore structures. While the industry still largely relies on highly empirical design charts and designer judgment to estimate the trajectory and capacity of the anchors, the simplified analytical models including the limit equilibrium and plastic limit analyses present huge steps forward in improving the design.

The objective of this thesis is to present the framework of a simplified plastic limit analysis to predict the capacity of drag embedment anchors in soft clays. The model is based on the plastic limit analyses assuming steady state behavior, and it makes the simplifying assumption that the anchor will quickly rotate and align such that any

forces at the padeye will pass through the anchors θ_{fs}. This model will then be verified against a series of published design charts and field tests.

As the presence of layered soil presents a significant challenge to the analysis of the trajectory of DEAs, the model will then be extrapolated to allow for the inclusion of a stiff layer of clay. Utilizing a simplified area transformation, equivalent to the embedment of the anchor in the stiff layer, the framework will allow the model to describe the behavior of the anchor as it transitions into the layer. Due to the lack of non-proprietary installation data, this model is unable to be validated, and will only provide example simulations to show expected behavior.

2. BACKGROUND

2.1 General DEA Behavior

2.1.1 Mooring Configurations

Floating offshore structures typically transfer their forces to the seabed through mooring lines and anchors. The mooring lines can consist of segments of chain, wire, and polyester rope, depending on the specific application. Those lines are typically arranged in one of two mooring configuration: catenary, and taut, as seen in Figure 2.

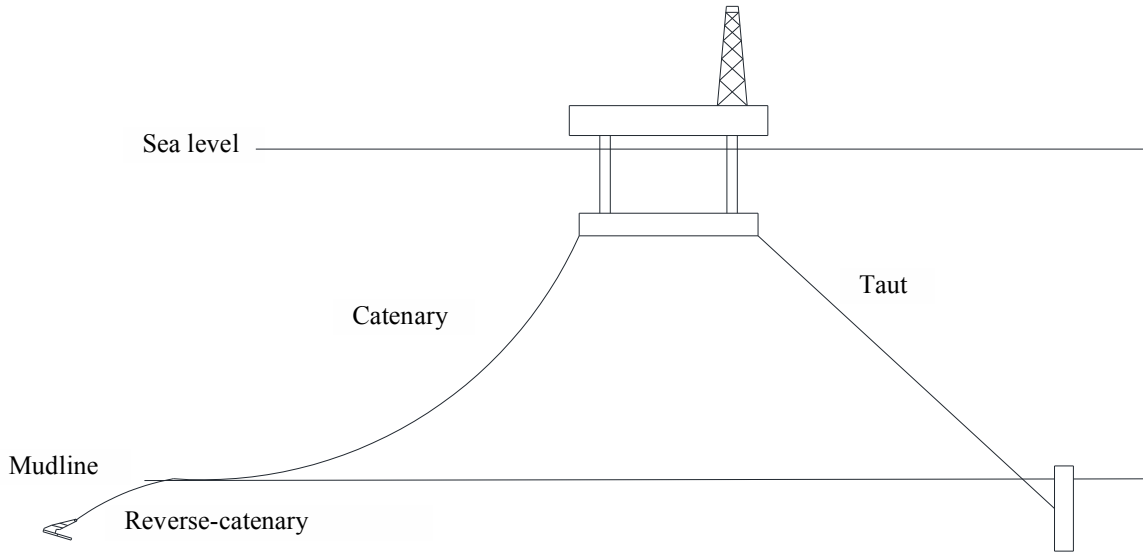

Figure 2: Mooring Configurations

In a catenary mooring systems the lines are typically heavy and extending a large distance outwards from the structure. The lines form an upwards concave or catenary shape in the water column reaching the seabed at a near horizontal angle. As the line

extends into the seabed, the curvature reverses and takes on a downward concave or reverse-catenary shape. Thus, the loads experienced at the anchor are largely horizontal, experience small vertical components. Catenary mooring systems are the ideal configuration for DEA.

In taut configurations the line held under tension and extend from the structure to the seabed typically at angles ranging from 30-45 degrees. This reduces the outward extent of the mooring system from the structure, decreasing the required length of mooring lines and reducing their contribution to the loads. As such it is often employed in deep and ultra-deep waters, but results in a significant vertical component to the anchor loads that are not suitable for DEA, but is acceptable for a VLA.

2.1.2 Basic Geometry

The basic geometry of a DEA consists of four components, fluke, shank, padeye, and forerunner as shown in Figure 3. The fluke acts as the resistance bearing component of the anchor and is equipped with fins and stabilizer to prevent pitch and yaw as the anchor embeds. The shank is designed to aid in the installation of the anchor and can also provide addition bearing capacity. The angle between the shank and the fluke has a significant impact on the behavior of the anchor and is a key element in the design of the anchor. The padeye is where the forerunner is connected to the shank typically using a shackle. The forerunner is the portion of the mooring line that is embedded into the seabed, and typically consists of either a chain or a wire cable.

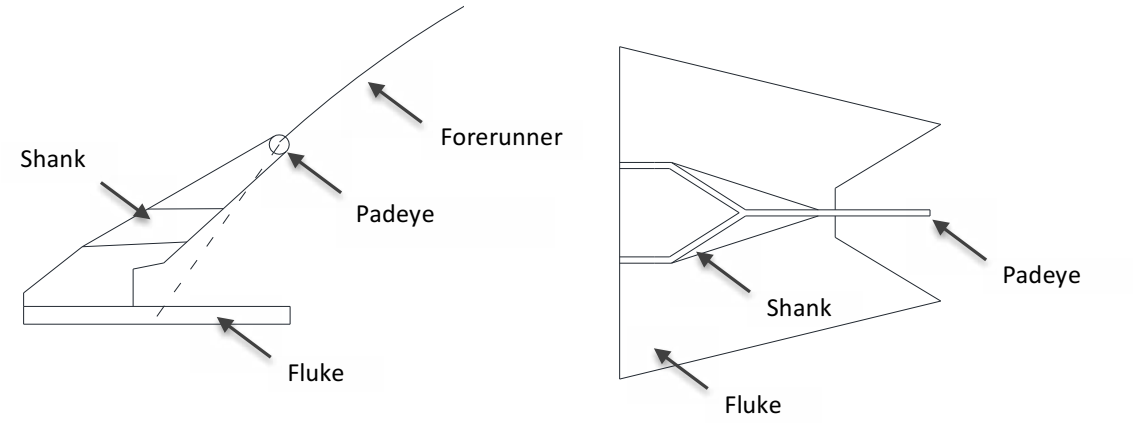

Figure 3: Anchor Components

2.1.3 Drag Anchor Behavior

DEAs refer to large anchors that are installed by lowering them to the seabed and dragging into place using an anchor handling vessel (AHV). As they dive into the seabed they rotate from a steep angle near the surface and gradually approach horizontal as they near their maximum resistance or ultimate holding capacity, UHC.

The anchors have been widely used for temporary moorings for mobile offshore drilling units (MODU). They have been used for permanent mooring to a much lesser extent, due to uncertainty in their installation. They provide an attractive solution as they are highly efficient, capable of supporting loads up to 33-55 time their weight (Vryhoff, 2010), and can provide significant cost savings due to decreased vessel costs and installation times. For temporary moorings the anchor can be retrieved at significantly lower loads, as low as 20-30% in soft clays (Vryhoff, 2010), by loading the anchor out of plane. In soils with limited available data they can be installed and proof loaded to capacity without presenting significant risk to the structure.

Anchors are manufactured to fit the projects needs and can vary in weight from less than 1 mT to upwards of 65 mT, with dimensions up to 6 m (fluke length) by 10 m to padeye, 11 m wide and 5m tall.

DEAs are designed to resist horizontal loads at the seabed using catenary mooring systems. When loaded out of plane of the shank or with large vertical loads they can have significant reductions in capacity. In sands and stiff clays they may only embed up to 1 to 2 fluke lengths, and maintaining a catenary system is vital to avoid pulling out the anchors. In soft clays DEA typically achieve a deep embedment ranging from 8-10 fluke lengths.

Depending on the soil type DEA will typically be configured in one of three fluke-shank settings. In soft clays the anchors set into the soil relatively easily and a high fluke shank angle typically around 50^{o} is desirable, as it helps maximize the capacity by keeping the loading angle closer to normal to the fluke. In sands and stiff clays anchors may experience difficulty in setting in and trip along the surface at larger fluke shank angles. Therefore, the fluke-shank angle is typically set at 30^{o}, even though it results in lower capacity. In addition to these two angles, some anchors are equipped with intermediate settings for angles for conditions between stiff soil and soft clays such as layered soils.

When deep embedment can be expected a VLA can be employed and a taut mooring system used. VLAs are an adaptation on a DEAs to allow them to resist vertical force components. To achieve this the VLA is installed in two stages. In the first stage, commonly referred to as installation, the anchor is installed like a DEA. In the second

stage, commonly referred to as loading, the mooring line is raised to an angle of approximately 40^o and rapidly loaded to break a shear pin and allow the free rotation of the shank. This allows the shank to align to a larger fluke-shank angle increasing the capacity and creating the ability to resist vertical loads.

2.2 Analysis Methods

A number of methods have been developed to predict the capacity of drag anchors. Generally, they can be grouped into one of four methods. The four methods are the efficiency method, empirical design charts, limit equilibrium solutions, and plastic limit analyses (PLA).

2.2.1 Efficiency Method

The efficient method estimates an anchors holding capacity by characterizing its efficiency ratio, e, also called it holding-capacity-to-weight-ratio. The ratio is defined by:

$$e = \frac{H_m}{W_A} \tag{2.1}$$

$where;$
$e = efficiency\ ratio$
$H_m = Ultimate\ horizontal\ holding\ capacity$
$W_A = Weight\ of\ anchor\ in\ air$

The anchor capacity can simply be estimated by multiplying its weight by the anchors efficiency. Values of e can be provided by the anchor manufacturer. This method serves as a historic method for estimating the capacity of anchors and should not be used for

more than a rough estimate of sizing to be followed with more rigorous solutions, though it is still largely employed by the U.S. Navy (Naval Facilities, 2012). The method does nothing to address specific configuration of the anchor, or the site specific soil characteristics. The holding capacity is extrapolated based upon the anchors weight which is known to be a poor measure as the capacity is more closely related to fluke area. As such the efficiency method has shown to significantly overestimate the capacity of large anchors (Naval Facilities, 2012).

2.2.2 Empirical Design Charts

The empirical design charts are most commonly used method for estimating the capacity of DEA. Each type of anchor has its own design chart that is the result of series of field tests conducted by anchor manufacturers, industry projects and the Naval Civil Engineering Laboratory. Depending on the chart, it can provide a variety of information from ultimate holding capacity (UHC), to estimations of drag, and penetration. The charts typically relate UHC capacity anchor weight on a log-log scale relying on the power law method which is expressed by:

$$H_m = \mathrm{m}(\mathrm{W}_A)^b \tag{2.2}$$

$where;$
$H_m = ultimate\ horizontal\ holding\ capacity$
$W_A = weight\ of\ anchor\ in\ air\ (kips)$
$m, b = dimensionless\ anchor\ constants$

The early charts provided by the Navel Civil Engineering Laboratory (NCEL 1987) provided only ultimate holding capacity estimates, based on broad soil classifications.

The two soil classifications are; soft soils for clays and silts, and hard soils for sands and stiff clays. Adjustments for soil type are made by varying the value of m, some examples of recommended power law method constants can be seen in

Table 1, and published Navy charts can be seen in Figure 4 and Figure 5.

Table 1: NCEL Recommended Design Chart Value Examples (NCEL, 1987)

Anchor	Soft Soils		Hard soils	
	m	b	m	b
Boss	210	0.94	270	0.94
Bruce Twin Shank	189	0.92	210	0.94
Danforth	87	0.92	126	0.80
Stevpris	189	0.92	210	0.94

These design charts still leave a wide range of uncertainty in estimating the capacity of DEAs, and do not provide estimates of the penetration or drag of the anchors, which are important for the installation of the anchor. Factors not included in the Navy charts, such as embedded mooring line type (chain or wire), and line diameter have a large impact on the trajectory and subsequently the capacity of DEA. More detailed design charts that include estimates of penetration and drag have been created by manufacturers such as design charts published by Vryhof Anchors for the Stevpris Mk6, as seen in

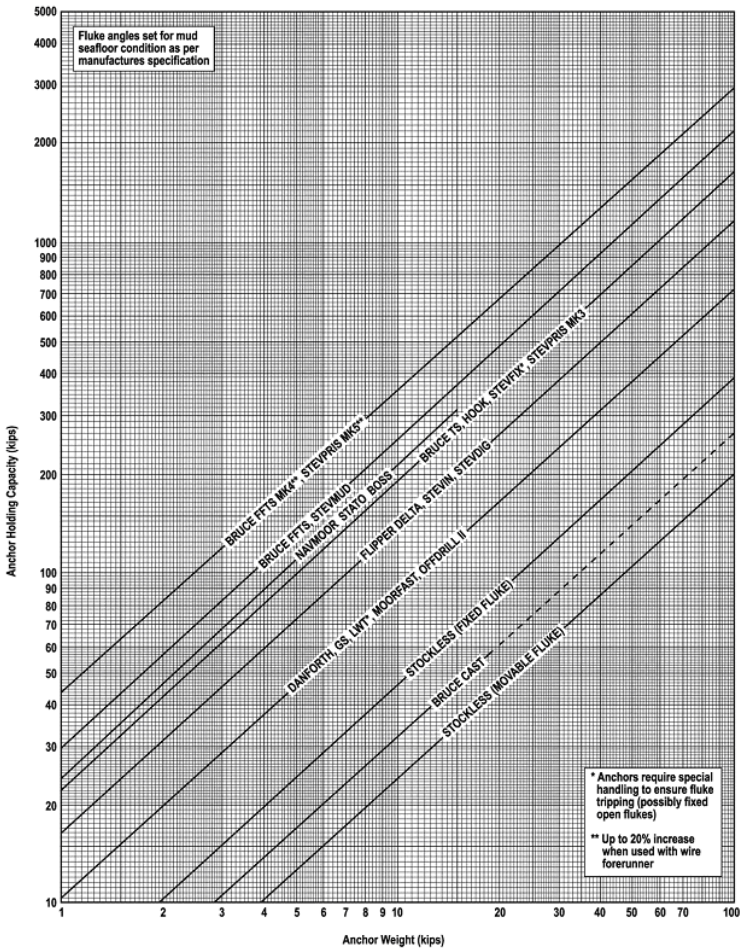

Figure 4: Design Charts for Soft Soils (Reprinted From NAVFAC, 2012)

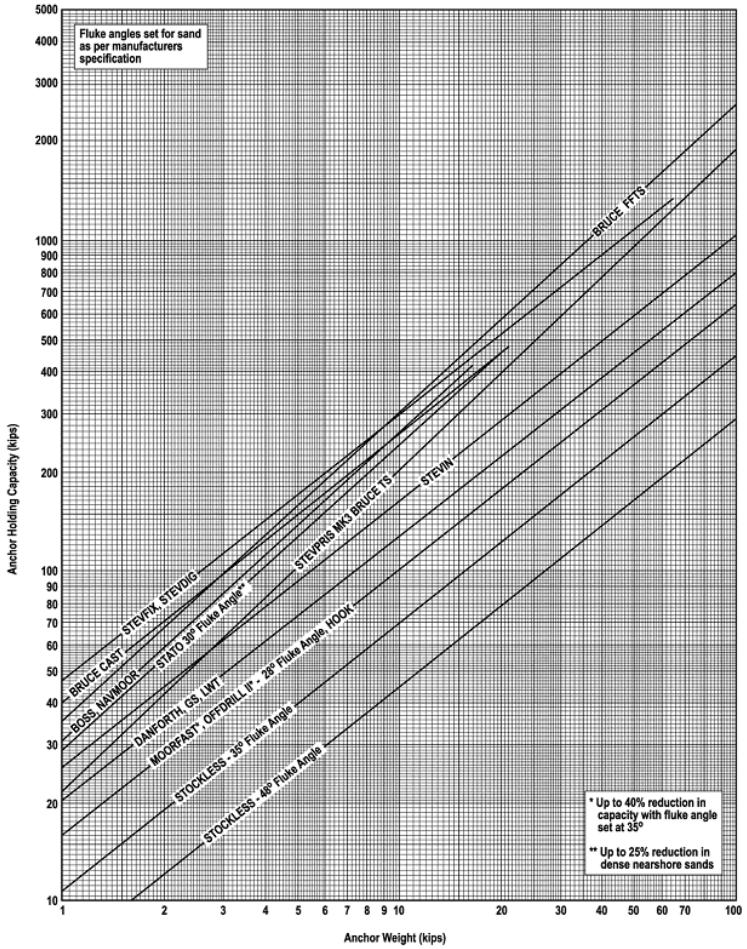

Figure 5: Design Charts For Hard Soils (Reprinted From NAVFAC, 2012)

Figure 6. Along with the design chart are tabular estimates of the estimates of capacity, drag, and penetration normalized by their UHC as the anchor embeds in the soil, as shown in Table 2. The effects of chain configuration as seen in some design charts such as those published by Bruce Anchors. A Bruce design chart for the FFTS Mk4 can be seen in Figure 7.

Table 2: Vryhof Trajectory Estimates (Vryhof, 2010)

Capacity/UHC, %	Drag/Max Drag, %	Penetration/Max Penetration, %
70	48	80
60	37	68
50	27	55
40	18	42
30	9	23

Not all design charts utilize the power law method or the weight of the anchor to estimate the capacity of the anchor. The design chart published by Vryhof for the Stevmanta VLA relates ultimate holding capacity, UHC, to the fluke area of the anchor through a series of two equations. It is important to note this anchor is a VLA so capacity is no longer limited to the horizontal direction. First the penetration is calculated using Equation 2.3 and then used to calculate its bearing capacity similar to an embedded plate using the Equation 2.4. Instead of using broad classification categories these equations allow for the inclusion of more anchor specific geometries, and site specific soil data. An example of a published Stevmanta chart can be seen in Figure 8.

$$z = 1.5 * k^{0.6} * b^{-0.7} * A_f^{0.3} * \tan^{1.7} \theta_{fs} \quad (2.3)$$

where;
$z = vertical\ penetration$
$k = shear\ strength\ gradient$
$b = moorling\ line\ diameter$
$A_f = fluke\ area$
$\theta_{fs} = fluke\ shank\ angle$

$$UPC = \mathrm{N}_c * s_u * A_{af} \tag{2.4}$$

$where;$
$UPC = ultimate\ pullout\ capacity$
$N_c = bearing\ capacity\ factor$
$s_u = undrained\ shear\ stress\ at\ depth\ (k * z)$
$A_f = fluke\ area$

While a significant improvement over the efficiency ratio method, the use of empirical charts are still deficient in many respects. Soils are characterized in broad undescriptive soil categories. The charts are highly empirical and still relate capacity to the weight of the anchor, when it is known to be a poor measure of anchor performance. The field tests which the curves are based on consist mainly of small anchors using chair forerunners extrapolated to larger sizes due to the costs associated with acquiring AHV large enough to test the largest anchor sizes to capacity. Capacities, penetration, and drag are presented at ultimate their configurations, which is undesirable as anchors are seldom installed to their ultimate capacity as any unexpected load would result in significant drag.

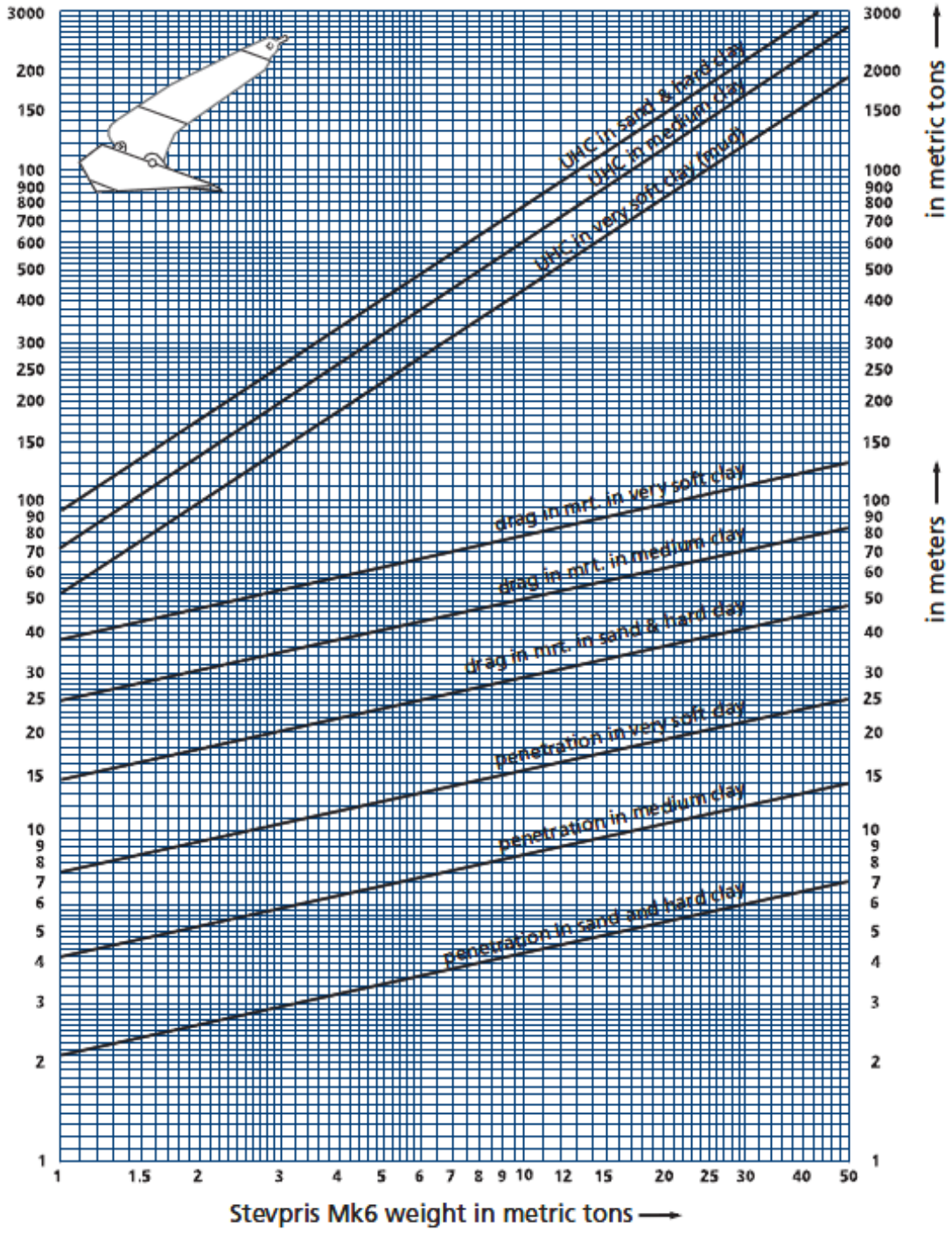

Figure 6: Strevpris Mk 6 Design Chart (Reprinted From Vryhof, 2010)

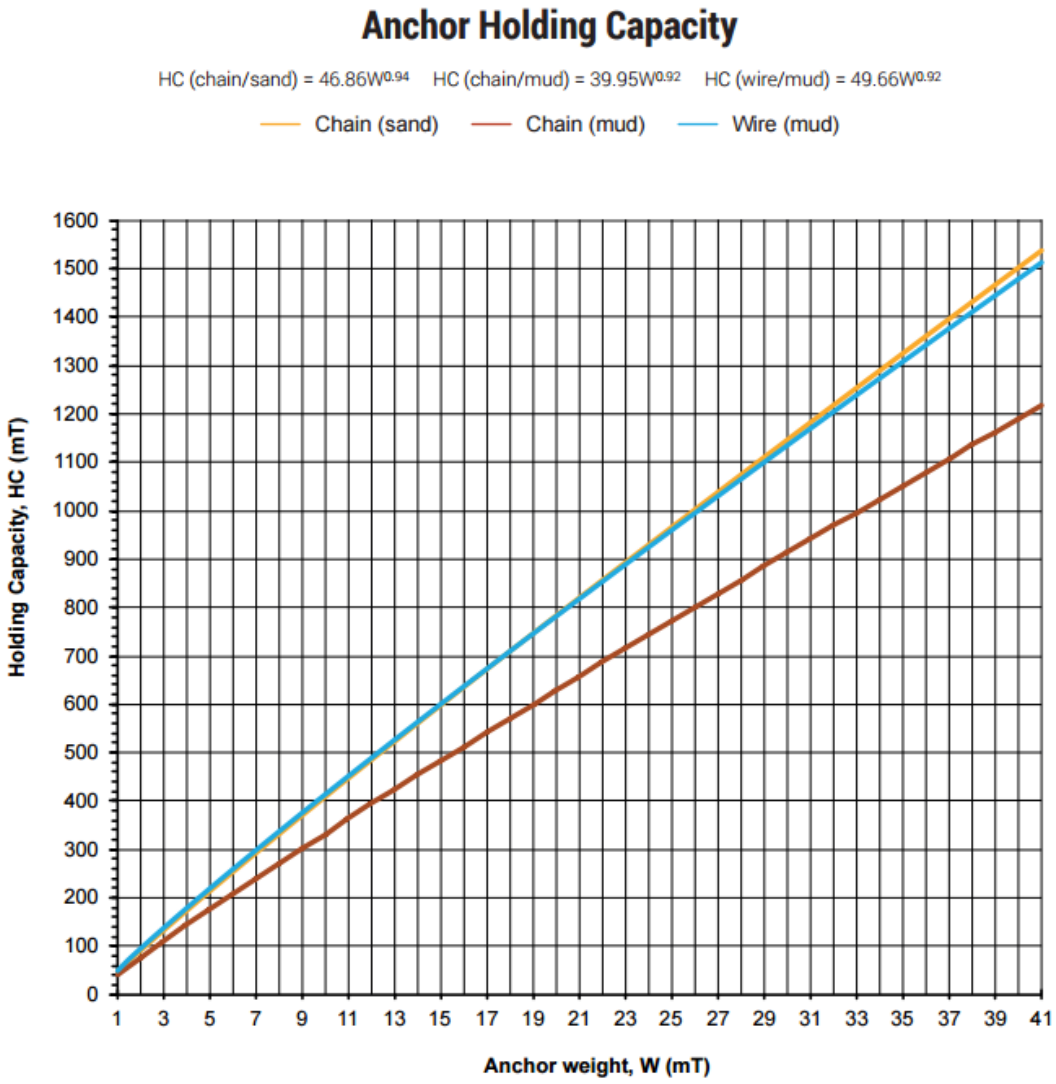

Figure 7: Bruce Anchors FFTS Mk 4 (Reprinted From Bruce, n.d.)

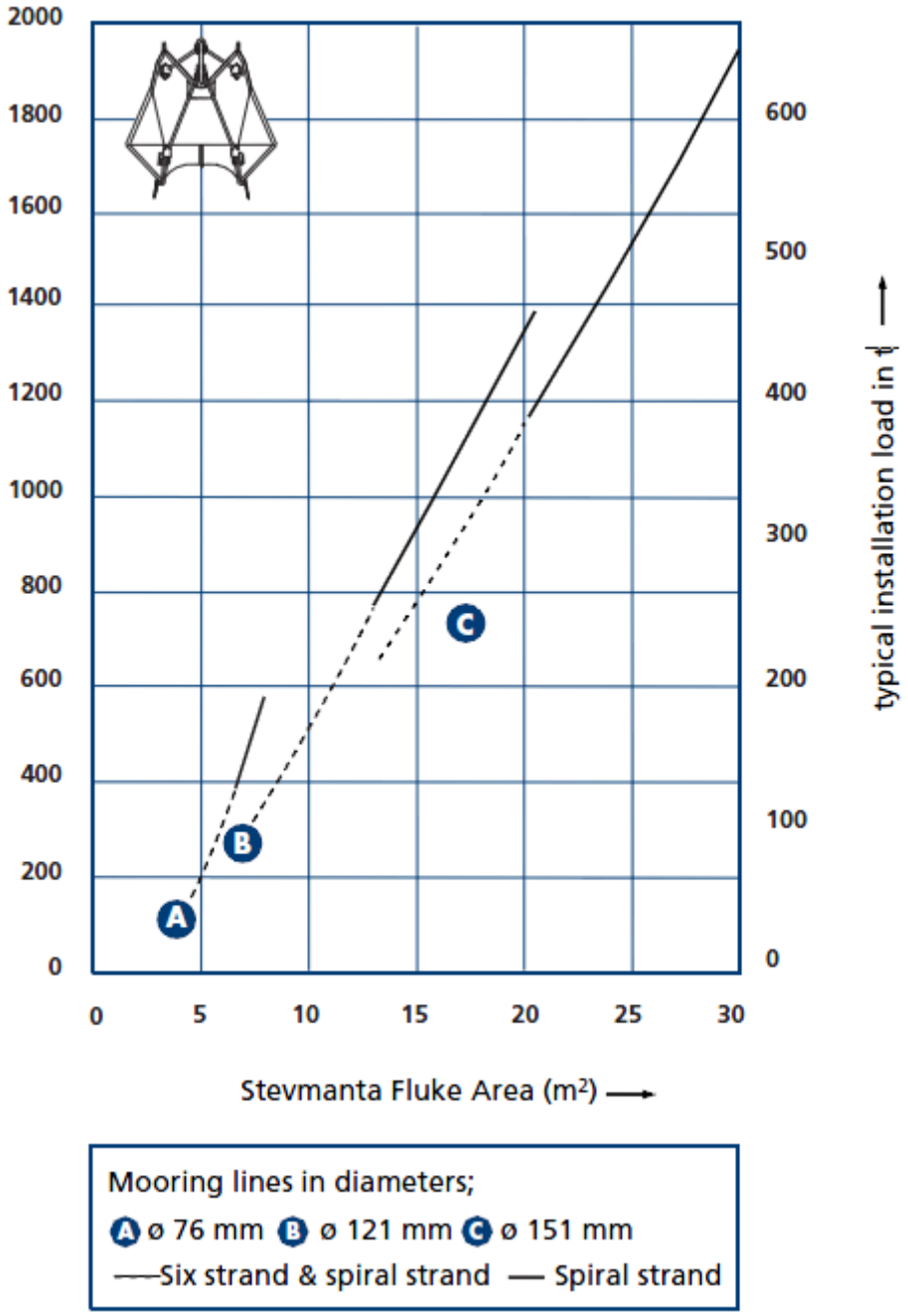

Figure 8: Stevmanta Design Chart Example (Reprinted from Vryhof, 2010)

2.2.3 Limit Equilibrium Solutions

The limit equilibrium models incorporate analytical solutions with geotechnical principles to estimate the trajectory and capacity of DEA as they are embedded into the seafloor. In the method the anchor is incrementally advanced while balancing the forces, and moments acting on the anchor at each step through rotation of the fluke. The various formulations of the limit equilibrium solutions each rely on different methods for estimating the forces acting on the anchor, and rotation mechanism.

The limit equilibrium solution for the capacity and trajectory in soft cohesive soils was first proposed by Stewart (1992). Subsequent variations of the limit equilibrium were proposed by Neubecker and Randolph (1996a), Dahlberg (1998) and Thorne (1998).

The Stewart (1992) method proposed a balancing the forces and moments formed along each anchor component. The forces were divided into the contributions from the anchor line, fluke, and shank, and further divided into components of shear and normal resistance. Each incremental displacement generally resulted in an unbalanced moment about the padeye, and anchor was rotated until equilibrium was satisfied.

The Neubecker and Randolph (1996a) method introduced a closed form analytical solutions to describe the behavior of the mooring line in relation to soil strength, anchor resistance and line angles at the anchor and the mudline where:

$$\frac{T_a}{2}(\theta_a^2 - \theta_0^2) = z\bar{Q} = zE_n N_c b\left(s_{uo} + \frac{kz}{2}\right) \tag{2.5}$$

$where;$
$T_a = padeye\ resistance$
$\theta_a = padeye\ line\ angle$
$\theta_0 = mudline\ line\ angle$
$z = padeye\ depth$
$\bar{Q} = average\ bearing\ resistance$
$E_n = forrunner\ type\ multiplier\ (chain = 2.5, wire = 1)$
$N_c = chain\ bearing\ factor\ (10)$
$b = forruner\ diameter$
$s_{uo} = mudline\ shear\ strength$
$k = shear\ strength\ gradient$

The resistance of the anchor could be calculated using the bearing capacity equation, then broken up into components based on the geometry of the anchor. The force parallel to the fluke could be found using the bearing factor equation:

$$T_P = fA_p N_c s_u \tag{2.6}$$

$where;$
$T_p = parallel\ resistantance$
$f = friction\ factor$
$A_P = projected\ frontal\ area$
$N_c = bearing\ factor$
$s_u = undrained\ shear\ strength$

The force then can be resolved up into components using a geometric characteristic of the anchor $\theta_{w,}$ which is found through back calculation of model tests:

$$T_W = \frac{T_P}{\cos \theta_W} \tag{2.7}$$

$where;$
$T_W = total\ anchor\ resistance$
$T_p = parallel\ resistance$
$\theta_W = geometric\ characterstic\ angle$

To maintain moment equilibrium the fluke will align to a geometric configuration described by:

$$\theta_a = \theta'_W - \beta \tag{2.8}$$

$where;$
$\theta_a = padeye\ line\ angle$
$\theta'_W = modified\ resultant\ angle$
$\beta = fluke\ angle$

Limit equilibrium solutions for sand presents an additional challenge as the assumption of a deeply embedded anchor becomes unreasonable with shallow anchor penetration. Shallow embedment typically results in a failure mechanism that extends to the surface. The capacity in sand was proposed by Lelievre and Tabatabee (1981) for an anchor wished in place to a given depth but trajectories coupled with capacities were not proposed until the refinement and the proposal of a kinematic model based on the principal of minimal work by Neubecker and Randolph (1996 b, c).

The solutions for sand (Neubecker and Randolph, 1996 b,c) and cohesive soils (Neubecker and Randolph, 1996 a) were combined and adapted to layered soils by

O'Neill (2000). To account for the transitional behavior between models it introduced fluke tip force, and relied on an arbitrary shift between sand and cohesive models once the anchor embedded midway through the fluke.

While the limit equilibrium provided a substantial step forward in terms of reducing the level of empiricism and using geotechnical principles a number of empirical constants remained such as f, and θ_w for the Neubecker and Randolph model.

2.2.4 Plastic Limit Solutions

The use of plastic limit analysis for the behavior of DEA was first proposed by O'Neill et al (2003). Refinements to the method were proposed by Aubeny et al (2005), and Aubeny and Chi (2010). The method is based on the concept that in soft soils the failure of the soil is result of localized plastic flow around the anchor. If the loading is assumed to be a combination of the vertical, horizontal and rotational load, as show in Figure 9, the behavior of the anchor can be described by the macro plastic yield locus combining the normal and tangential forces as well as the moment loads the anchor experiences.

$$f(F_n, F_t, M) = 0 \tag{2.9}$$

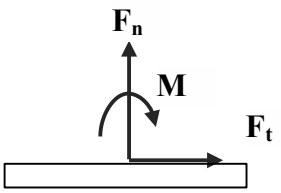

Figure 9: Loading Components

The shape of the yield surface was investigated using upper bound analyses (O'Neill 2003) for conditions of maximum non-interactive behavior, and through the use of two dimensional finite element analysis for interactive behavior. Since the full 3D modeling of the anchors would be very time consuming and anchor specific the geometry was simplified to a 2D rectangular plate. To evaluate the interaction behavior the plate was displaced through a series of load combination using an undrained Tresca soil until it reached capacity. The results over a range of load combinations were then fit to an equation using the method of least squares. The results showed the general shape of the yield locus can be described by the Murff (1994) equation:

$$f = \left(\frac{F_n}{F_{n\,max}}\right)^q + \left[\left(\frac{M}{M_{max}}\right)^m + \left(\frac{F_t}{F_{t\,max}}\right)^n\right]^{1/p} - 1 = 0 \tag{2.10}$$

$where;$
$f = yield\ function$
$F_n, F_t, M = normal, tangential, and\ moment\ loads$
$F_{n\,max}, F_{t\,max}, M_{max} = maximum\ load\ values$
$q, m, n, p = interaction\ coeffients$

The maximum capacities found by upper bound analysis were:

$$N_n = \frac{F_{n\,max}}{L_f s_u} = 3\pi + 2 + 2\frac{t_f}{L_f}\left(\alpha + \frac{1+\alpha}{\sqrt{2}}\right) \tag{2.11}$$

$$N_t = \frac{F_{t\,max}}{L_f s_u} = 2\left(\alpha + N_{tip}\frac{t_f}{L_f}\right) \approx 2\alpha + 15\frac{t_f}{L_f} \tag{2.12}$$

$$N_m = \frac{M_{max}}{L_f^2 s_u} = \frac{\pi}{2}\left[1 + \left(\frac{t_f}{L_f}\right)^2\right] \quad (2.13)$$

$where;$
N_n, N_t, N_m = uniaxial bearing factors
$L_f = fluke\ length$
$t_f = fluke\ thickness$
$\alpha = adhesion\ factor$
$N_{tip} = tip\ bearing\ factor$

In addition to the analysis conducted by O'Neill (2003), Murff et al. (2005) and Yang et al. (2008) investigated the shape of the yield surface and found the interaction coefficients shown in Table 3. An example of the yield locus using the Murff et al (2005) coefficients can be seen in Figure 10.

Table 3: Yield Locus Interaction Coefficients

Study	m	n	p	q
O'Neill et al (2003)	1.37	3.74	1.22	3.68
Murff et al (2005)	1.56	4.19	1.57	4.43
Yang et al (2008)	1.40	3.49	1.31	4.14

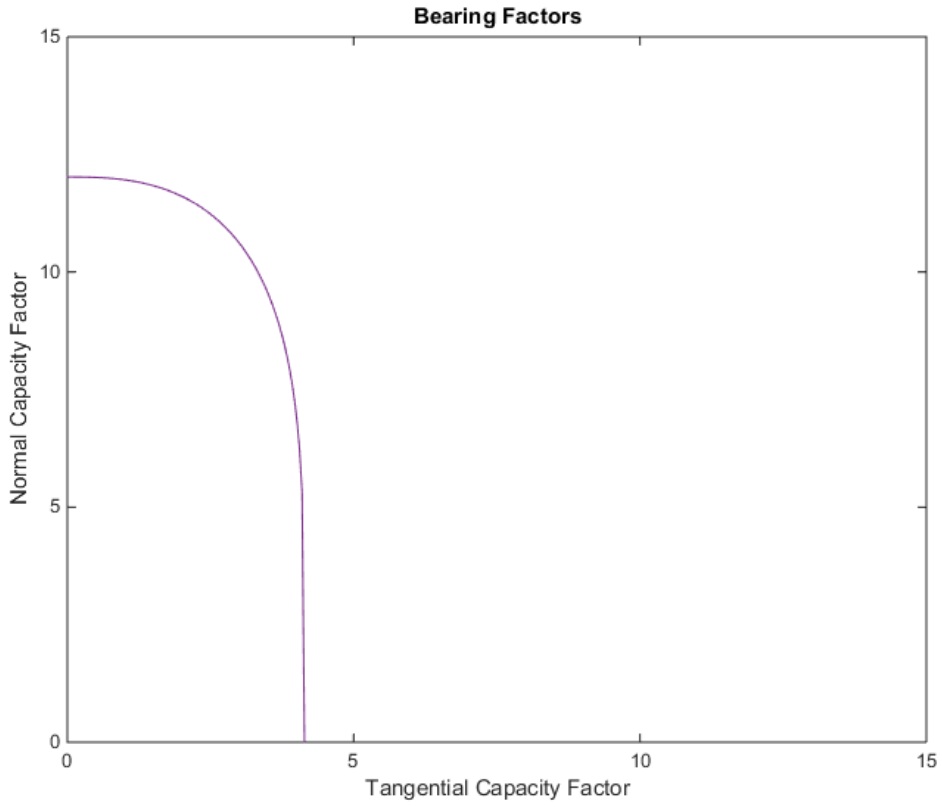

Figure 10: Yield Locus Using Murff et al (2005) Coefficients

Since during installation the anchor will continually be in a state of failure, and assuming undrained associated flow ratios of the motion of the anchor can be described by the normality of the yield surface at failure:

$$\frac{\delta v}{\delta t} = \frac{\partial f}{\partial N} \Big/ \frac{\partial f}{\delta T} \tag{2.14}$$

$$\frac{\delta \beta}{\delta t / L_f} = \frac{\partial f}{\partial \left(M / L_f \right)} \Big/ \frac{\partial f}{\partial T} \tag{2.15}$$

Using incremental displacements, the normal and rotational increments become:

$$\Delta n = \frac{\partial f}{\partial N} \Big/ \frac{\partial f}{\delta T} \Delta t \tag{2.16}$$

$$\Delta \beta = \left[\frac{\partial f}{\partial \left(M / L_f \right)} \Big/ \frac{\partial f}{\partial T} \right] \frac{\Delta t}{L_f} \tag{2.17}$$

The initial method proposed by O'Neill (2003) proposed the following analysis:

1. Assume an initial fluke and depth
2. Assume a padeye tension, T_a
3. Calculate padeye chain angle using Equation 2.5
4. Using the geometry break the padeye tension into its components of F_n, F_t, M
5. Check if forces are on the yield surface, if not return to Step 2
6. Assume a tangential displacement and calculate the normal and rotational displacements using Equation 2.16 and 2.17
7. Update the anchor coordinates
8. Repeat Steps 2-7 until β=0

Aubeny et al (2005) and Aubeny et al (2008) suggested estimating T_a based through an upper bound virtual work analysis. During each increment the center of rotation is optimized to determine the minimum collapse load for a given orientation. Coupled with solutions for the evolution of θ_a with respect to depth (Equation 2.9) this provides a unique load and orientation for each step.

$$\frac{d\theta_a}{dz} = \frac{1}{\theta_a}\left(\frac{E_n N_c b}{T_a} - \frac{k(\theta_a^2 - \theta_o^2)}{2s_{uo}}\right) \tag{2.18}$$

$where;$
$d\theta_a = change\ in\ padeye\ angle$
$dz = change\ in\ penetration$
$E_n = forrunner\ type\ multiplier\ (chain = 2.5, wire = 1)$
$N_c = chain\ bearing\ factor\ (10)$
$b = forruner\ diameter$
$k = shear\ strength\ gradient$
$\theta_a = padeye\ line\ angle$
$\theta_o = mudline\ line\ angle$
$T_a = padeye\ resistance$
$s_{uo} = mudline\ shear\ strength$

The Aubeny and Chi (2010) model took the framework provided by O'Neill et al (2003) and using the geometry of the anchor developed a method to estimate, T_a, based on the geometry of the angle between the fluke and T_a. The change in θ_a is estimated using Equation 2.9, and the fluke is rotated according the normality of the yield surface. The change in θ_a then calculated through successive iterations of Equation 2.9. The anchor is then displaced and the process is repeated until the anchor approaches a horizontal angle.

3. UNIFORM SOIL MODEL

The analysis proposed here is for estimating the trajectory and capacity of drag embedment anchors in homogeneous cohesive soil based on a simplified plastic limit analysis. Based on the plastic limit method proposed by O'Neill et al (2003) the model assumes that the failure of the soil can be described by the undrained plastic flow around the anchor. As such the behavior of the soil can be described by a macro yield locus that relates the tangential, F_t, normal, F_n, and moment, M, loads on the anchor. The kinematic behavior of the anchor is based on an incremental advancement of the anchor and the relative components are calculated from the resulting plastic strains in the soil around the anchor.

This model is a simplified version of the model proposed Aubeny and Chi (2010) that takes advantage of their conclusion that the anchor rapidly approaches an equilibrium state where the padeye angle, θ_a, aligns with the fluke shank θ_{fs}, resulting in the fluke and the θ_a rotating at the same rate and a condition of zero moment. Therefore the yield locus can be reduced to a two dimensional slice of the full yield locus where M=0, and the rotation of the anchor can be described by the rotation of θ_a.

$$f(F_n, F_t) = 0 \tag{3.1}$$

The model allows for the inclusion of small increases in s_u with depth, the objective of this analysis is to provide a simplified analysis that then can be expanded to account for the inclusion of stiff layers of clay in the soil profile.

3.1 Idealized Anchor Geometry

The geometry of the idealized anchor consists of four main components a forerunner, padeye, shank, and fluke. The general anchor configuration can be seen in Figure 11 and Figure 12.

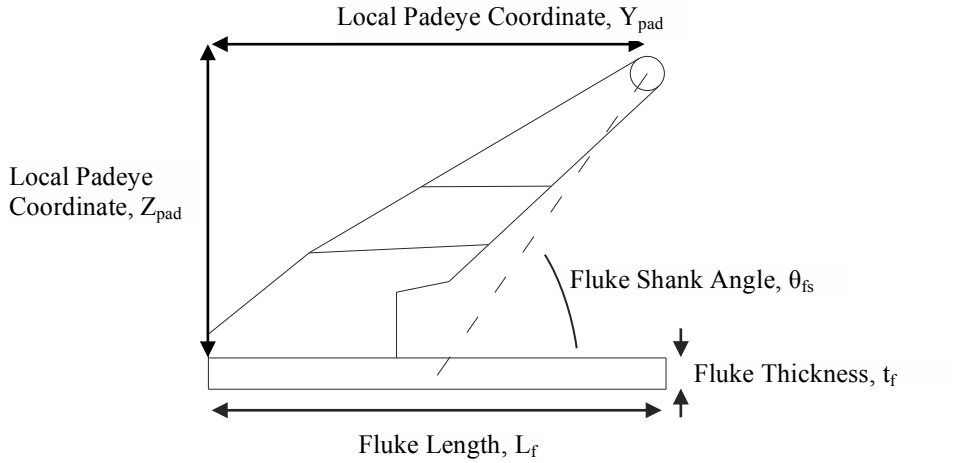

Figure 11: Anchor Geometry

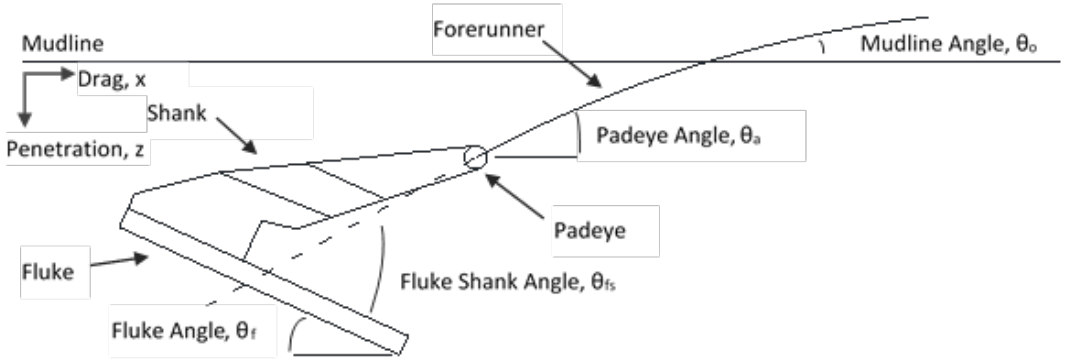

Figure 12: Anchor Configuration

The forerunner is the portion of the mooring cable that is embedded into the soil along with the anchor. It has a diameter, b, and can be made of either chain or wire cable. While chain forerunners provide additional frictional capacity along the line compared to wire forerunners, they typically reduce the embedment of the anchor due to increased normal resistance along the line resulting in lower overall capacity. The angle that the line forms with the seabed is called the mudline angle, θ_o, and the line angle from horizontal at the padeye is called the padeye angle, θ_a. The reaction force in the forerunner at the mudline is the mudline tension, T_o, and the reaction force at the padeye is called the padeye tension, T_a.

The padeye is where the forerunner is connected to the shank of the anchor using a shackle. The padeye is located at a distance parallel to the fluke from the rear of the anchor, y_{pad}, and perpendicular, z_{pad}. The shank is the portion of the anchor protruding from the fluke. This model assumes a thin shank that will not mobilize bearing resistance. The fluke is the bearing component of the DEA with an area, A_f. While modern DEA have a range of complex geometric shapes the formation of the yield locus for plastic limit analysis relies on the use of rectangular flukes with a fluke length, L_f. In order to use the general yield locus framework, the geometry is converted into an equivalent rectangular fluke that maintains the same first moment of area about its natural axis, y_{na}, as seen in Figure 13. The location of the y_{na}, the equivalent length, L_{fe}, and equivalent width, W_{fe}, can be found by Equation 3.1-3.3. The thickness of the fluke, t_f, is defined as the average thickness of the projected frontal area of the fluke.

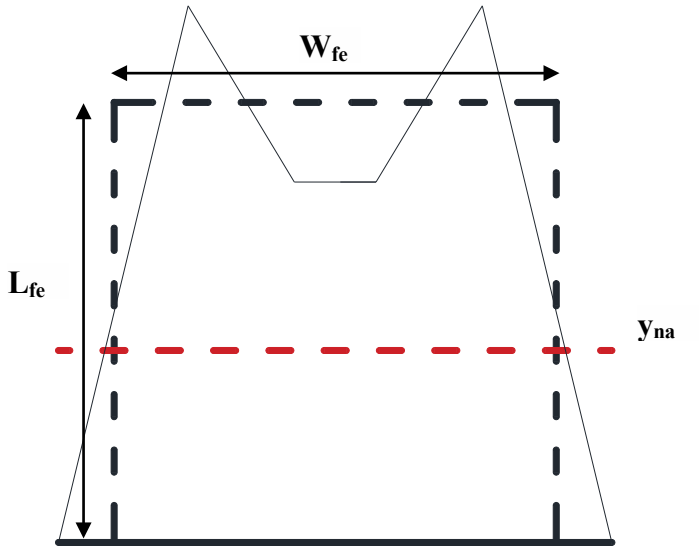

Figure 13: Equivalent Rectangular Anchor

$$y_{na} = \frac{\int dA_f}{A_f/2} \tag{3.1}$$

$$L_{fe} = \frac{4}{A_f} \int y_{na} dA_f \tag{3.2}$$

$$W_{fe} = \frac{A_f}{L_{fe}} \tag{3.3}$$

where;
$y_{na} = distance\ to\ the\ neural\ axis$
$A_f = fluke\ area$
$L_{fe} = equivalent\ idealized\ anchor\ length$
$W_{fe} = equivalent\ idealized\ anchor\ width$

The angle the padeye forms with the fluke is referred to as the fluke-shank angle, θ_{fs}.

The definition of θ_{fs} has varied widely between models from measuring the angle

between the padeye and the fluke at rear of the anchor, to the anchors center of gravity, or even just the angle the shank makes with the anchor. In this model as it plays a critical role in the behavior of the DEA the θ_{fs} is defined as the angle between the padeye and the fluke at the neutral axis.

$$\theta_{fs} = \tan^{-1} \frac{z_{pad}}{y_{pad} - y_{na}} \tag{3.4}$$

$where;$
$\theta_{fs} = fluke\ shank\ angle$
$z_{pad} = local\ z\ coordinate\ to\ the\ padeye$
$y_{pad} = local\ y\ coordiante\ to\ the\ padeye$
$y_{na} = distance\ to\ the\ neutral\ axis$

3.2 Yield Surface

Assuming localized undrained plastic flow the behavior of the anchor will be controlled by the anchors yield locus. Since the soil will continually be in a state of failure, assuming associated flow and that displacements are the result of plastic strains the relative displacements can be estimated by the normality of the location on yield surface.

Under the assumption of steady state behavior, T_a, will align with the θ_{fs}. Therefore no moment will result on the anchor and the yield locus can be reduced to Equation 3.5 as seen using the Murff et al (2005) coefficients in Table 3.

$$f = \left(\frac{F_n}{N_{n\,max}}\right)^q + \left[\left(\frac{M}{M_{max}}\right)^m + \left(\frac{F_t}{N_{t\,max}}\right)^n\right]^{\frac{1}{p}} - 1 \tag{3.5}$$

$$= \left(\frac{F_n}{F_{n\,max}}\right)^q + \left(\frac{F_t}{F_{t\,max}}\right)^{n/p} - 1 = 0$$

$where;$
$N_n, N_t, M = normal, tangential, moment\ bearing\ factors\ on\ the\ anchor$
$F_{nmax}, F_{tmax}, M_{max} = maximum\ bearing\ factors$
$q, m, n, p = dimensionless\ constants$

The values of N_{tmax}, and N_{nmax} are found using the analytical solutions provided by O'Neill et al (2003) presented here again:

$$N_{nmax} = \frac{F_{n\,max}}{L_f s_u} = 3\pi + 2 + 2\frac{t_f}{L_f}\left(\alpha + \frac{1+\alpha}{\sqrt{2}}\right) \tag{3.6}$$

$$N_{tmax} = \frac{F_{t\,max}}{L_f s_u} = 2\left(\alpha + N_{tip}\frac{t_f}{L_f}\right) \approx 2\alpha + 15\frac{t_f}{L_f} \tag{3.7}$$

$where;$
$N_{nmax} = maximum\ normal\ bearing\ factor$
$N_{tmax} = maxium\ tangentail\ bearing\ factor$
$s_u = undrained\ shear\ strength$
$t_f = fluke\ thickness$
$L_f = equivalent\ fluke\ length$
$\alpha = adhesion$
$N_{tip} = Tip\ bearing\ factor$

The ratio of the normal to tangential motion, R_{nt}, found by taking the appropriate partial derivatives of the yield surface, can then also be reduced to:

$$R_{nt} = \frac{v_n}{v_t} = \frac{dn}{dt} = \frac{(N_{tmax}/N_{nmax})\left(\frac{pq}{n}\right)}{[(|N_m|/N_{mmax})^m + (|N_t|/N_{tmax})^n]^{\frac{1}{p}-1}} \frac{(|N_n|/N_{nmax})^{q-1}}{(|N_t|/N_{tmax})^{n-1}} \quad (3.8)$$

$$= \frac{(N_{tmax}/N_{nmax})\left(\frac{pq}{n}\right)}{[(|N_t|/N_{tmax})^n]^{\frac{1}{p}-1}} \frac{(|N_n|/N_{nmax})^{q-1}}{(|N_t|/N_{tmax})^{n-1}}$$

$where;$
$R_{nt} = ratio\ of\ normal\ to\ tangential\ motion$
$v_n = normal\ velocity\ component$
$v_t = tangential\ velocity\ component$
$F_n, F_t, M = Normal, tangential, Moment\ loads\ on\ the\ anchor$
$F_{nmax}, F_{tmax}, M_{max} = maxium\ bearing\ factors$
$q, m, n, p = dimensionless\ constants$

Using an incremental advance parallel to the anchor, ds, the change in penetration (depth), and the change in drag (horizontal) as seen in Figure 14 can be calculated from the fluke angle:

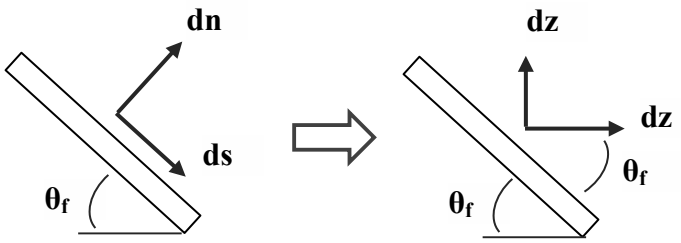

Figure 14: Displacement Components

$$dz = ds * \sin(\theta_f) - ds * R_{nt} * \cos(\theta_f) \tag{3.9}$$

$$dx = ds * \sin(\theta_f) - ds * R_{nt} * \cos(\theta_f) \tag{3.10}$$

$where;$
$dz = vertical\ displacement\ component$
$dx = horizontal\ displacement\ component$
$ds = incrementally\ advanced\ tangential\ displacement\ component$
$\theta_f = fluke\ shank\ angle$

The adhesion between the anchor and soil assumes a completely remolded condition and can be estimated using:

$$\alpha = \frac{1}{s_t} \tag{3.11}$$

$where;$
$\alpha = adhesion$
$s_t = soil\ sensitivity$

3.3 Mooring Line Equations

The behavior of the mooring line and subsequently the rotation of the anchor will be controlled the Neubecker and Randolph (1996a) equations presented again here as Equation 3.12 & Equation 3.15. Using Equation 3.12 the initial value of θ_a can be calculated, and under the assumption of steady state condition θ_a will align with $\theta_{fs,}$ and the two will rotate as at the same rate about the padeye allowing θ_f to be calculated using Equation 3.13.

$$\frac{T_a}{2}(\theta_a^2 - \theta_0^2) = z\bar{Q} = 2bN_cE_n\left(s_{uo} + \frac{kz}{2}\right) \tag{3.12}$$

$$\theta_f = \theta_{fs} - \theta_a \tag{3.13}$$

$where;$
$T_a = padeye\ tension$
$\theta_o = mudline\ line\ angle$
$\theta_a = padeye\ line\ angle$
$z = padeye\ depth$
$\bar{Q} = average\ bearing\ resistance$
$b = forruner\ diameter$
$E_n = forrunner\ type\ multiplier\ (chain = 2.5, wire = 1)$
$N_c = chain\ bearing\ factor\ (10)$
$s_{uo} = mudline\ shear\ strength$
$k = shear\ strength\ gradient$
$\theta_f = fluke\ angle$
$\theta_{fs} = fluke\ shank\ angle$

Due to the θ_f rotating at the same angle as θ_a to keep in alignment the rotation of the fluke $\Delta\beta$ equal to the rotation $d\theta a$ can be described by Aubeny et al (2010) equation:

$$\Delta\beta = d\theta_a = \frac{1}{\theta_a}\left(\frac{E_nN_cb}{T_a} - \frac{k(\theta_a^2 - \theta_o^2)}{2s_{uo}}\right)ds \tag{3.14}$$

$where;$
$\Delta\beta = change\ in\ fluke\ angle$
$d\theta_a = change\ in\ line\ angle\ at\ the\ padeye$
$b = forruner\ diameter$
$E_n = forrunner\ type\ multiplier\ (chain = 2.5, wire = 1)$
$N_c = chain\ bearing\ factor\ (10)$
$s_{uo} = mudline\ shear\ strength$
$k = shear\ strength\ gradient$
$\theta_o = mudline\ line\ angle$
$\theta_a = line\ angle\ at\ the\ padeye$
$T_a = padeye\ tension$
$ds = incremental\ tangential\ advance$

Calculations of mudline capacity can be found using Equation 3.15

$$T_o = T_a \exp\left[\mu(\theta_a - \theta_o)\right] \tag{3.15}$$

$where;$
$T_o = mudline\ tension$
$T_a =$ padeye tension
$\mu = mooring\ line\ frictional\ coefficent\ (0.4 - 0.6)$
$\theta_o = mudline\ line\ angle$
$\theta_a = line\ angle\ at\ the\ padeye$

3.4 Capacity Calculations

The value of T_a is found using the bearing capacity equation:

$$T_a = N_e A_f s_u \tag{3.16}$$

$where;$
$T_a = padeye\ capacity$
$A_f = fluke\ area$
$N_e = effective\ bearing\ factor$
$s_u = undrained\ shear\ strength\ at\ the\ padeye$

To do this calculation the value of Ne must first be found. It can be calculated by breaking T_a into its components F_n, and F_t using the geometry of the anchor as show in Figure 15.

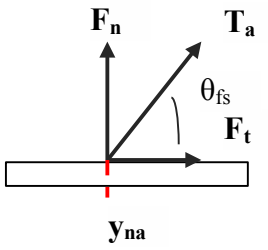

Figure 15: Forces Acting on the Anchor

(3.17)

$$F_n = T_a sin(\theta_{fs})$$

$$F_t = T_a cos(\theta_{fs}) \quad (3.18)$$

$where;$
$F_n = normal\ force\ acting\ on\ the\ fluke$
$F_t = tangential\ forcing\ acting\ on\ the\ fluke$
$\theta_{fs} = fluke\ shank\ angle$

Since the soil will be in a continual state of failure and therefore on the yield surface those components must lie on the yield surface. Substituting those values back into the function of the yield locus (Equation 3.5) it becomes Equation 3.5, which then can be solved for the value of N_e. Under a homogenous soil the value of N_e is constant during embedment.

$$f = \left(\frac{sin(\theta_{fs})N_e}{N_{n\,max}}\right)^q + \left(\frac{cos(\theta_{fs})N_e}{N_{t\,max}}\right)^{\frac{n}{p}} - 1 = 0 \quad (3.19)$$

$where;$
$f = equation\ of\ the\ yield\ locus$
$\theta_{fs} = fluke\ shankangle$
$N_e = effective\ bearing\ factor$
$N_{tmax}, N_{nmax} = maximum\ bearing\ factors$

3.5 Model Algorithm

The kinematic model for the DEA is based on an incremental advance of the anchor where the anchor is advanced a small distance, ds, parallel to the bottom of the fluke. The ultimate capacity of the fluke is reached when θ_f approaches zero.

1. Assume initial depth, z, at of the anchor at which it sets in
2. Calculate equivalent geometry, y_{na}, L_{fe}, and W_{fe}, using Equation 3.1-3.3
3. Calculate θ_{fs} using Equation 3.4
4. Calculate N_e using Equation 3.19, and T_a using Equation 3.16
5. Calculate the initial θ_a using Equation 3.12 and initial $\theta_{f,}$ using Equation 3.13
6. Calculate R_{nt} using Equation 3.8 and $\Delta\beta$ using Equation 3.14
7. Calculate dz, and dx using Equation 3.9 & 3.10
8. Update anchor location penetration, z, drag, x, and fluke angle $\theta_f=(\theta_{f\,(i-1)}-d\theta_a)$
9. Calculate T_o using Equation 3.15
10. Update θ_a ($\theta_{a=}\ \theta_{a,\,(i-1)}-d\theta_a$)
11. Repeat steps 5-10 until θ_f approaches zero

Typical outputs of the model for trajectory and capacity using the arbitrary fluke geometry shown in Figure 16 and the parameters outlined in in Table 4 can be seen in Figure 17 and Figure 18.

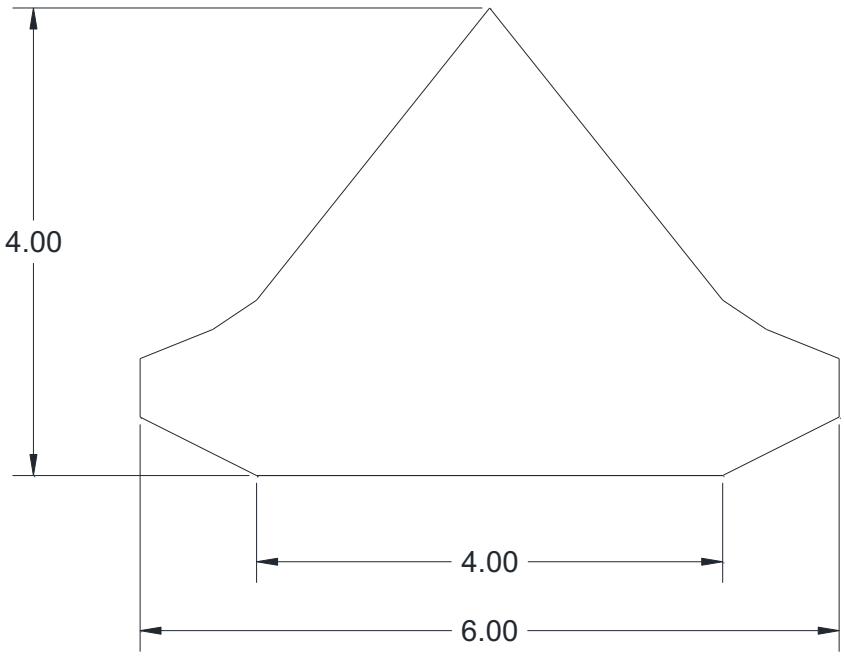

Figure 16: Example Geometry

Table 4: Example Model Properties

Property	Value
s_{uo}	4 kPa
k	1.5 kPa/m
S_t	3
b	89 mm
Forerunner type	Chain
y_{pad}	2.64 m
z_{pad}	3.36 m
m	1.56
n	4.19
p	1.57
q	4.43

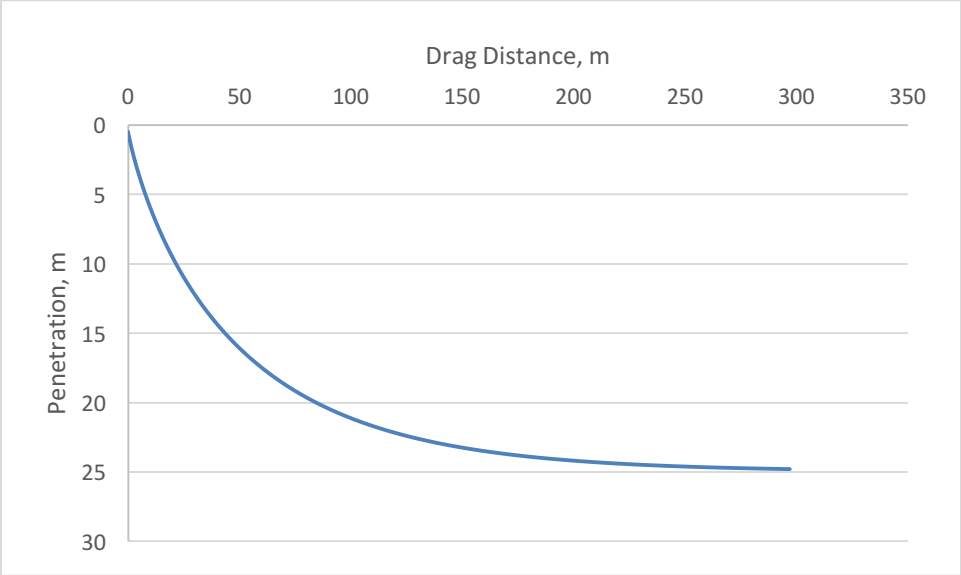

Figure 17: Typical Trajectory

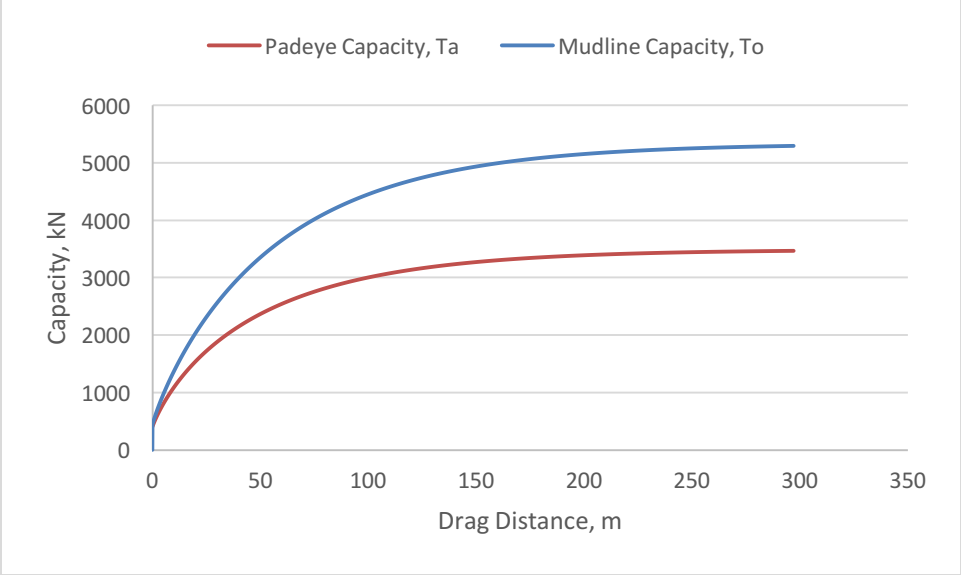

Figure 18: Typical Capacities

3.6 Validation

To provide a level of validation to the model the results of simulations were compared to manufacturer design charts and a series of field installations.

3.6.1 Empirical Charts

As the empirical design charts represent the industry standard for estimating the capacity of DEA the results of the model was compared to two manufacturer design charts. The results were compared for a variety of forerunner diameters (76mm, 121mm, 151mm) and types (chain, and wire). The two design charts selected were the Vryhoff Strevpris Mk5 and the Bruce FFTS. For the comparison to soft clay design charts the soil properties recommended by Vryhoff (2010) as show in Table 5.

Table 5: Soil Properties Chart Comparison

Parameter	Value
s_{uo}	4 kPa
k	1.5 kPa/m
S_t	2

3.6.1.1 Stevpris Mk5

The Stevpris Mk5 design charts (Vryhoff, 2010) provide the ultimate holding capacity, and estimates of the penetration of the anchor. The comparison of the ultimate holding capacity can be seen in Figure 19 and a comparison of the ultimate penetration in Figure 20.

The model estimated higher capacities for anchors with wire forerunners than the design chart, and lower values for chain forerunners. The wire results typically started

near the chart estimates then shifted to higher estimates as they neared their allowable capacity, while the chains initially resulted in low values but approached the chart solution as they neared their ultimate capacity. The two forerunner types bound the design chart estimates, indicating good agreement between the model and design chart. Additionally the range of this bound could be reduced by the use of intermediary chain diameters besides the three chosen for analysis.

The model showed higher penetration than the design charts for wire forerunners. Estimates with chain forerunners showed moderately good agreement with chart values.

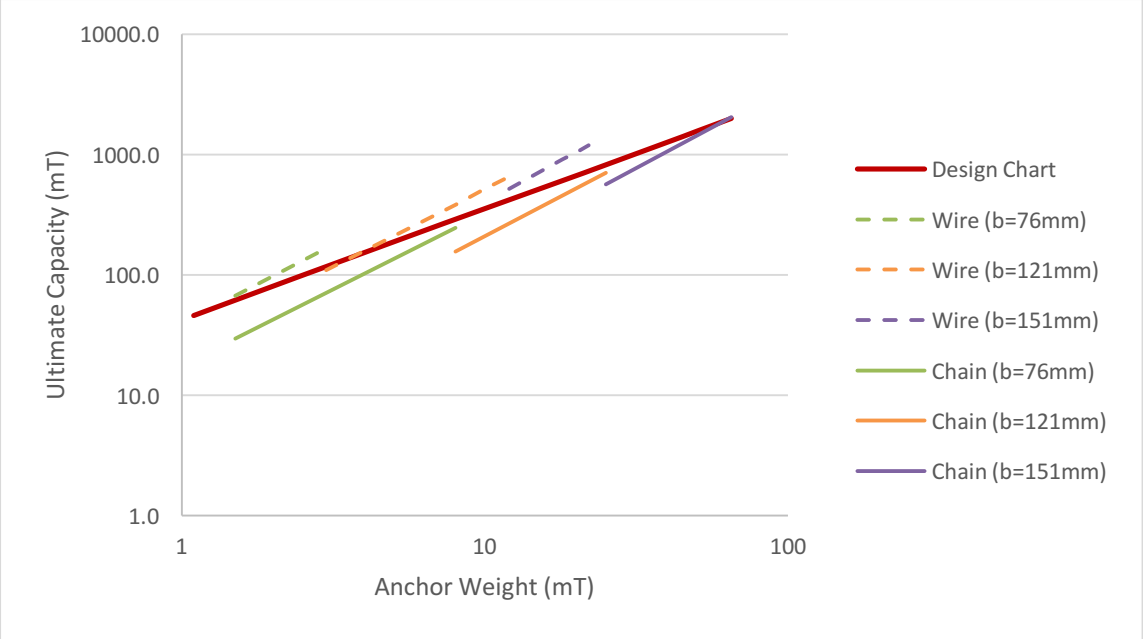

Figure 19: Stevpris Mk5 Capacity Comparison

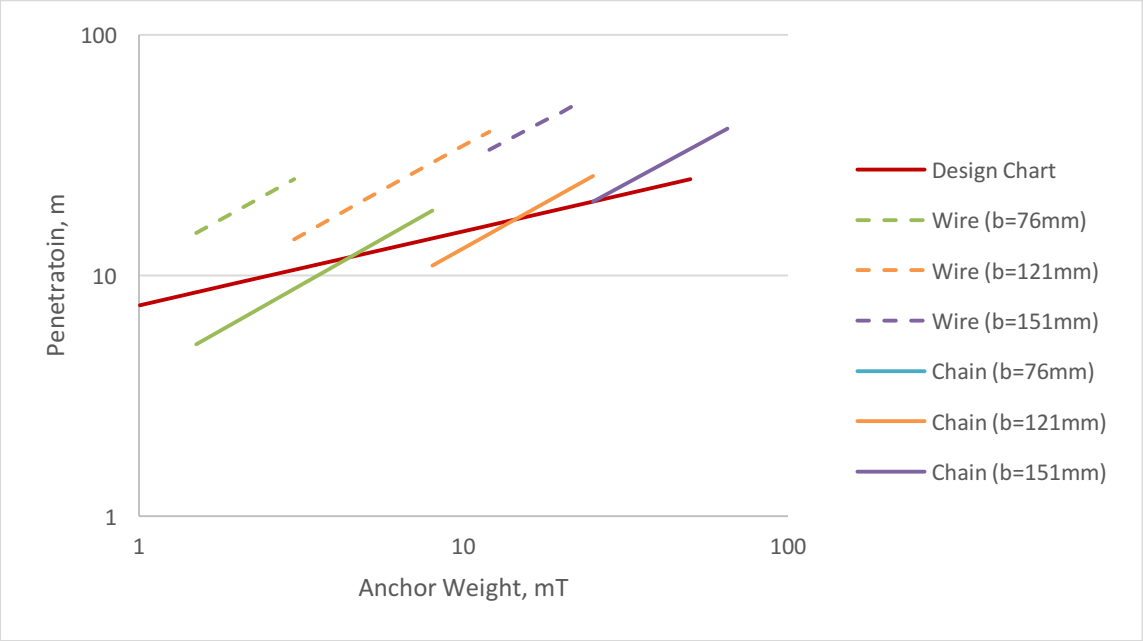

Figure 20: Stevpris Mk5 Penetration Comparison

3.6.1.2 FFTS Mk5

The Bruce FFTS Mk5 design charts (Bruce Anchors, n.d.) provide estimated capacities for both chain and wire forerunners. The comparison of the ultimate holding capacity for a wire forerunner can be seen in Figure 21 and chain forerunner in Figure 22.

Similar to the results for the Stevpris Mk5, the model again predicts a higher capacity when comparing wire forerunners and a lower capacity when predicting chain forerunners even with the separate design curves for wire and chain capacities. In general the chain does fit closer to the chart estimates than compared to the Stevpris chart.

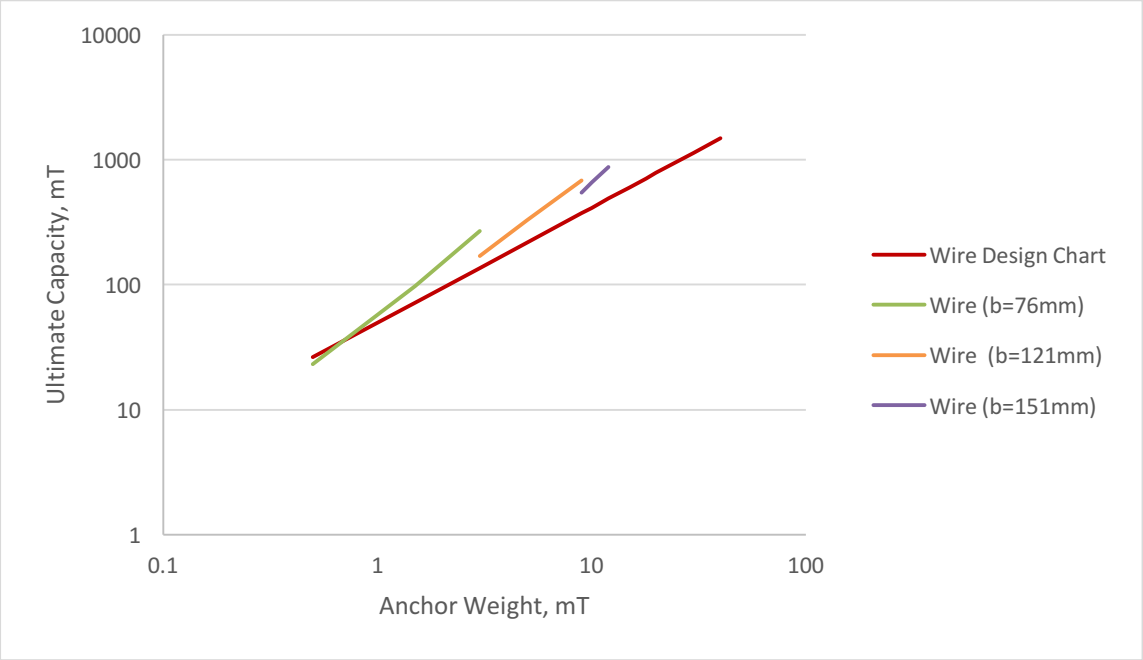

Figure 21: Bruce FFTS Mk5 Wire Comparison

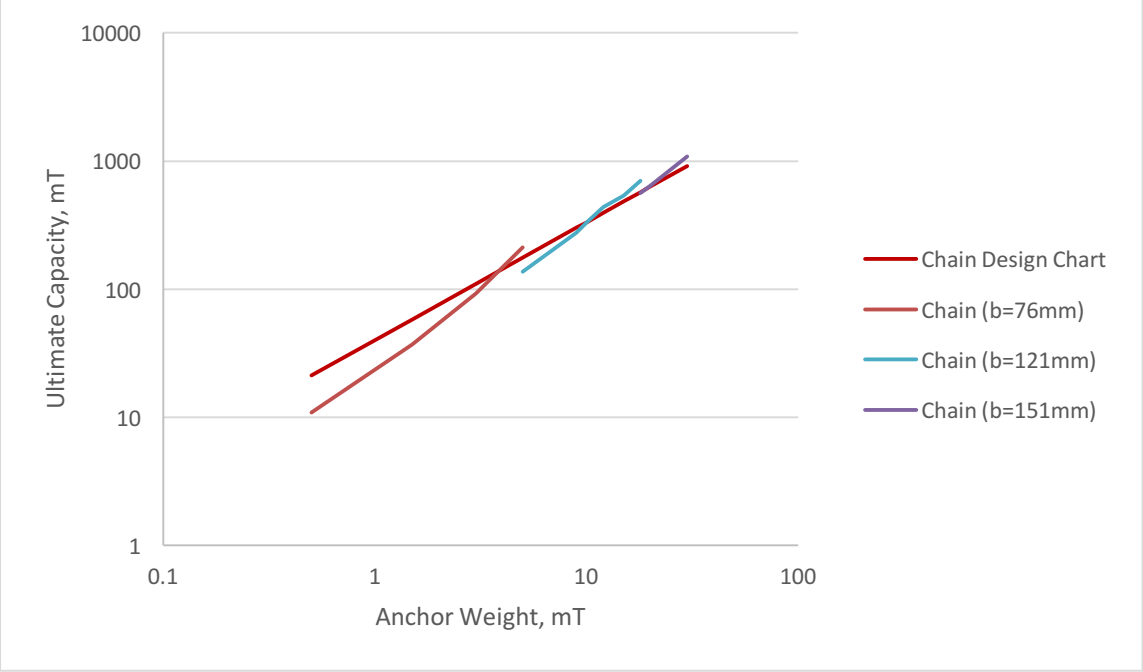

Figure 22: Bruce FFTS Mk5 Chain Comparison

3.6.2 Field Tests

The model was compared to a series of actual installations where the anchors were installed and the behavior recorded presented by Kim (2005). Due to these being recorded field data the amount of data recorded can vary significantly from a single data points, to continuous records of embedment depth and line tension.

3.6.2.1 South Timbalier Block 295 in the Gulf of Mexico

The trajectory and capacity of two anchors were measured during their installation at South Timbalier Block 295 in the Gulf of Mexico. In both cases the anchors were installed using wire forerunners with a chain diameter of 76mm. The Bruce Dennla Mk 2 and the Vryhoff Stevmanta are VLAs, which means the model will only be applicable to the installation phase of the anchor prior to the release of the shank. The results of the soil investigation can be seen in Table 6.

Table 6: South Timbalier Soil Properties

Property	Value
s_{uo}	0 kPa (0.01kPa used)
k	1.6 kPa/m
S_t	3

The installation of Dennla Mk2 (12.7 kN) recorded trajectory and capacity data during the entire installation. The comparison of the recorded data and the model can be seen in Figure 23 for the trajectory and Figure 24 for the capacity. During the installation three distinct phases can be seen; setting-in, penetration, and pull out. The setting in phase represents a transient phase as the anchor is setting into the soil and beginning to dive,

which is outside of the scope of this model. The penetration embedment is the same process as a DEA and making it a valid comparison to the model. Model calculations show good matches to measurements for both trajectory and capacity. The final phase represents pullout where the capacity of the anchor was exceeded and the anchor began to pull out of the soil.

The installation of the Vryhoff Stevmanta (31.16kN) recorded only one measurement of trajectory, but did collect tension data throughout the entire installation. The trajectory, as seen in Figure 25, shows the model slightly under predicted the embedment, while the tension (Figure 26) was slightly over predicted.

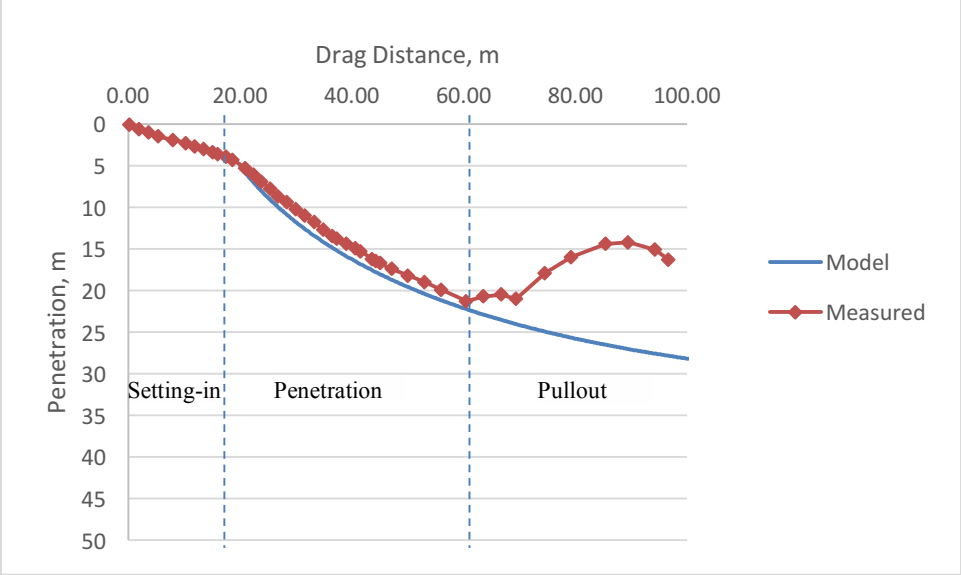

Figure 23: South Timbalier Trajectory Dennla

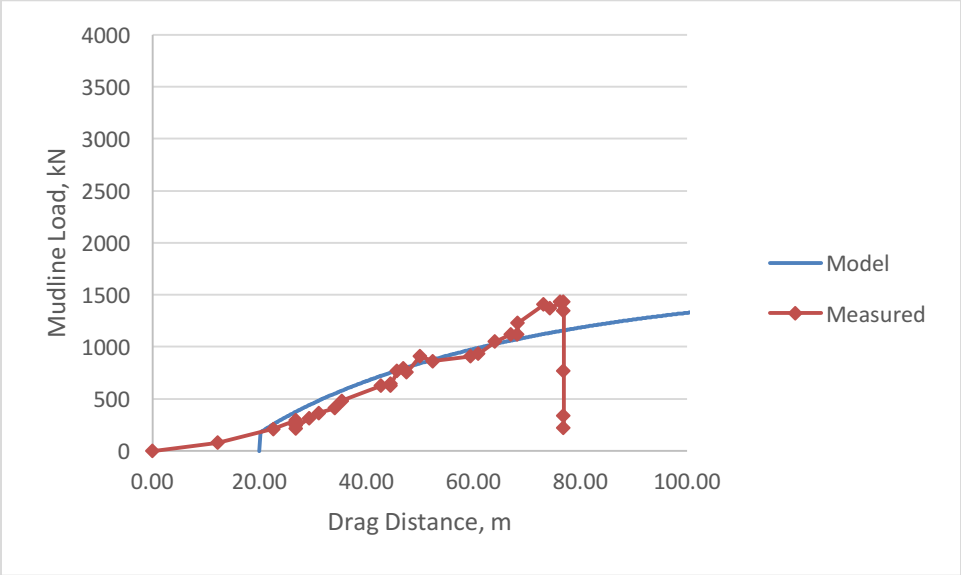

Figure 24: South Timbalier Capacity Dennla

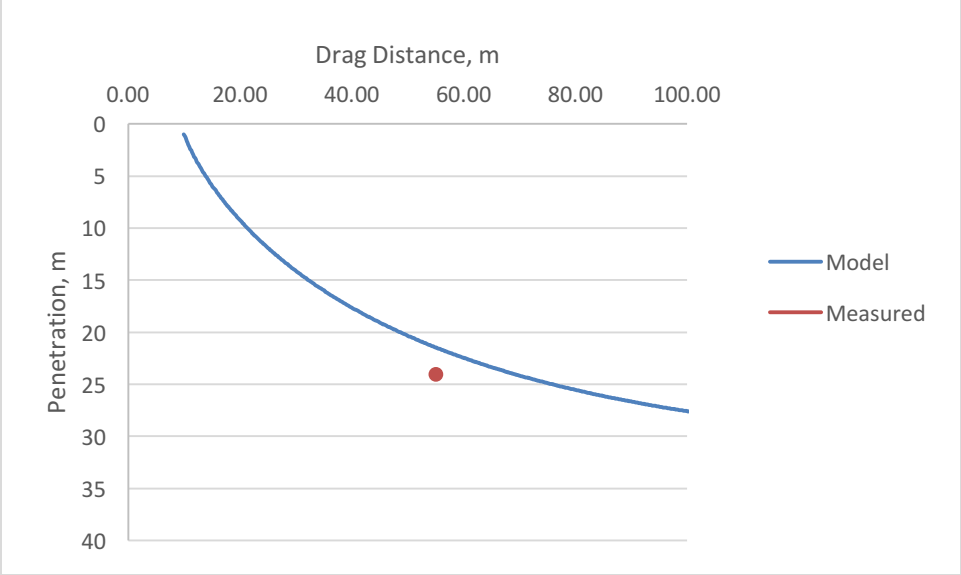

Figure 25: South Timbalier Trajectory Stevmanta

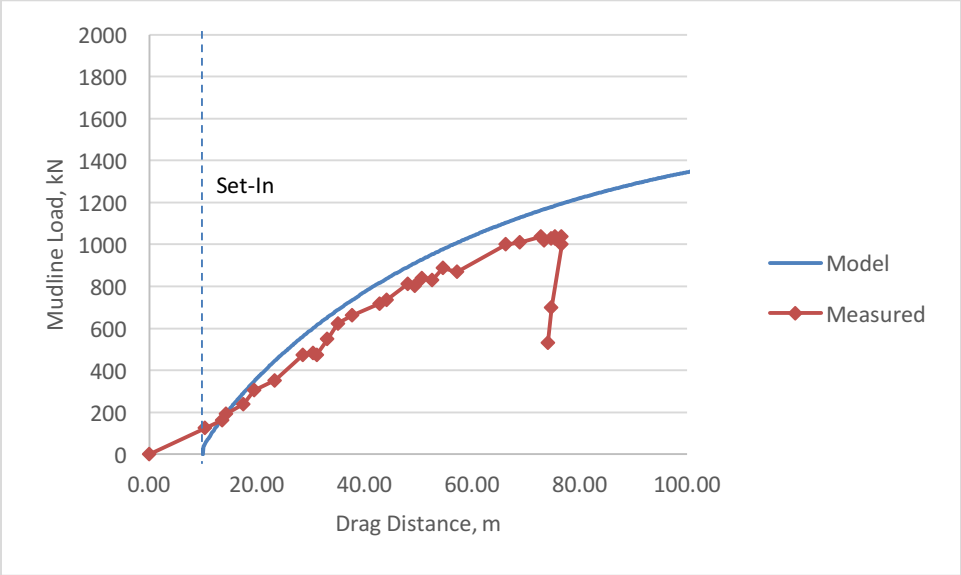

Figure 26: South Timbalier Capacity Stevmanta

3.6.2.2 Liuhua 11-1 Field

At the Liuhua 11-1 South China Sea field 11 Bruce FFTS Mk4 (392 kN) anchors were installed using chain forerunners with a diameter of 127mm. At this site a range of shear strengths were proposed, and estimates of S_t were not provided. As such, an average value of s_{uo} was used and S_t=3 was assumed, as shown in Table 7, which is a typical value for offshore soils. Using these values both the trajectory, Figure 27 and capacity Figure 28 show good agreement with the model.

Table 7: Liuhua Soil Properties

Property	Value
s_{uo}	6-12 kPa (9 kPa used)
k	1.6 kPa/m
S_t	3 (assumed)

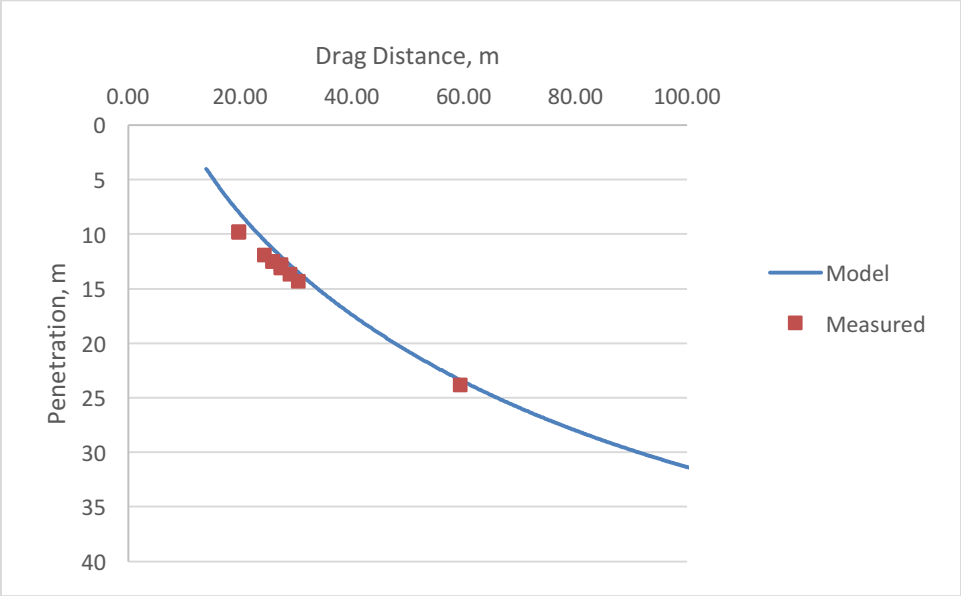

Figure 27: Liuhua Trajectory

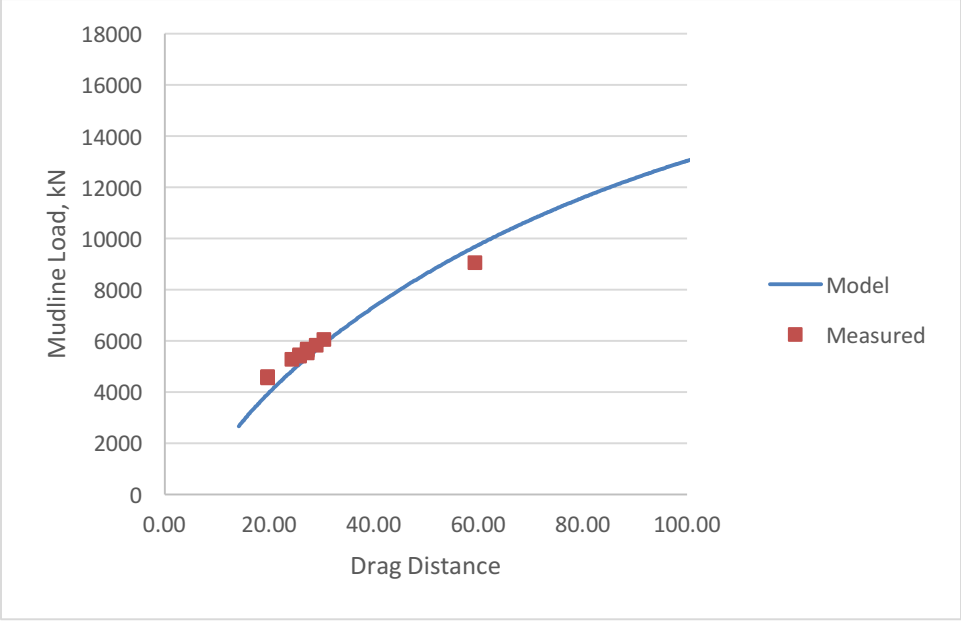

Figure 28: Liuhua Capacity

4. LAYERED COHESIVE SOIL

Layered soils present a significant challenge for the installation methods for DEAs. Design charts and most limit equilibrium and plastic limit analysis solution do not consider heterogeneity, aside from linear variation in strength. While the O'Neill (2000) model does introduce a tip resistance factor to help analyze the approach to the layer, it relies on an arbitrary shift between governing models as the DEA passes through the layer. This may not be representative of the transition as the anchor is partially embedded in the soil. Therefore, if layered soils are encountered, designers must rely on their judgment to estimate if the anchor will penetrate through a stiff layer. While the installation is backed up by proof loads during installation, it leaves a lot of uncertainty in the installation of anchors in layered soils.

The proposed model presents the framework for analyzing the capacity and trajectory of DEA as they embed in soft cohesive soils with stiff cohesive layers. The model, an extension of the model previously described in Section 4, is based on the premise the increases in shear strength while embedded in the stiff layer can be analyzed as an area transformation of the fluke area. This will allow the model to capture the behavior of the anchor as it embeds into the stiff soil.

4.1 Area Geometry

In the layered model the fluke is governed by the same equations as the base model except that the properties of the anchor, effective fluke area and first moment of the fluke area, are modified by the encounter with the stiff layer. As the anchor embeds into the stiff layer the embedded area will multiplied by a factor equal to the ratio of the

undrained shear strength of the stiff layer to the undrained shear strength of the base soil model, s_{ur}. Using this transformation the enhanced area of the fluke, A_{fe}, becomes:

$$A_{fe} = A_f + A_s(s_{ur} - 1) \tag{4.1}$$

where;
$A_{fe} = enhanced\ fluke\ area$
$A_f = actual\ fluke\ area$
$A_s = embeded\ fluke\ area$
$s_{ur} = shear\ strength\ ratio$

As the fluke embeds into the stiff layer the enhanced area and the location of the enhanced regions will continue to change as different regions of the fluke embed. This will results in a continual shift in the location of the neutral axis, y_{na}, and the equivalent geometry, W_{fe}, and L_{fe}.

$$y_{na} = \frac{\int dA_{fe}}{A_{fe}/2} \tag{4.2}$$

$$L_{fe} = \frac{4}{A_{fe}} \int y_{na} dA \tag{4.3}$$

$$W_{fe} = \frac{A_{fe}}{L_{fe}} \tag{4.4}$$

where;
$y_{na} = distance\ to\ the\ neural\ axis$
$A_{fe} = enhanced\ fluke\ area$
$L_{fe} = equivalent\ idealized\ anchor\ length$
$W_{fe} = equivalent\ idealized\ anchor\ width$

With y_{na} shifting as the anchor penetrates through the stiff layer θ_{fs} will also update at each increment in the stiff layer resulting in an additional component of fluke rotation as the new θ_{fs} aligns to θ_a.

$$\theta_{fs} = \tan^{-1} \frac{z_{pad}}{y_{pad} - y_{na}} \tag{4.5}$$

$where;$
$\theta_{fs} = fluke\ shank\ angle$
$z_{pad} = local\ z\ coordinate\ to\ the\ padeye$
$y_{pad} = local\ y\ coordiante\ to\ the\ padeye$
$y_{na} = distance\ to\ the\ neutral\ axis$

4.2 Yield Surface

The area transformation of the fluke will result in a change in the shape of the yield locus. Assuming the yield surface maintains the same general shape as Equation 3.5 the magnitude of the maximum bearing factors will increase according to the area transformations

$$N_{nemax} = \frac{F_{n\,max}}{L_{fe} s_u} = 3\pi + 2 + 2\frac{t_f}{L_{fe}}\left[\left(\alpha + \frac{1+\alpha}{\sqrt{2}}\right)\right] * N_{nmult} \tag{4.6}$$

$$N_{temax} = \frac{F_{t\,max}}{L_{fe} s_u} \approx 2\alpha + 15\frac{t_f}{L_{fe}} * N_{tmult} \tag{4.7}$$

$where;$
$N_{nemax} = enchanced\ normal\ bearing\ factor$
$F_{nmax} = maximum\ normal\ force$
$L_{fe} = equivalent\ fluke\ length$
$s_u = undrained\ shear\ strength$
$t_f = fluke\ thickness$
$\alpha = adhesion$

$N_{nmult} = enchanced\ fluke\ area\ multiplier$
$N_{temax} = enchanced\ tangential\ bearing\ factor$
$F_{tmax} = maximum\ tangential\ bearing\ factor$
$N_{tmult} = enchanced\ frontal\ area\ multilpier$

N_{nmult} will be the result of the increase in the fluke due to the transformation while N_{tmult} is the result of the increase in the projected frontal area of the fluke.

$$N_{nmult} = \frac{A_{fe}}{A_f} \tag{4.8}$$

$$N_{tmult} = 1 + \frac{w_{max\ stiff}}{w_{max}} \frac{(s_{ur} - 1)}{2} \tag{4.9}$$

$where;$
$A_{fe} = enchanced\ fluke\ area$
$A_f = real\ fluke\ area$
$N_{nmult} = enhanced\ fluke\ area\ multiplier$
$N_{tmult} = enchanced\ frontal\ area\ multiplier$
$w_{max\ stiff} = maximum\ enchanced\ width\ in\ stiff\ layer$
$s_{ur} = shear\ strength\ ratio$
$w_{max} = maximum\ real\ width$

Due to the constantly evolving maximum bearing factors while maintaining the same for the shape of the yield surface will continually distort during embedment. This will result in a constantly changing direction of plastic flow now calculated by:

$$R_{nt} = \frac{v_n}{v_t} = \frac{(N_{temax}/N_{nemax})(pq/n)}{[(|N_t|/N_{temax})^n]^{1/p-1}} \frac{(|N_n|/N_{nemax})^{q-1}}{(|N_t|/N_{temax})^{n-1}} \quad (4.10)$$

$where;$
$R_{nt} = ratio\ of\ normal\ to\ tangential\ motion$
$v_n = normal\ velocity\ component$
$v_t = tangential\ velocity\ component$
$N_n, N_t = normal, and\ tangential\ bearing\ factors$
$F_{nemax}, F_{temax} = maximum\ bearing\ factors$
$q, m, n, p = dimensionless\ constants$

4.3 Mooring Line Equations

Resistance along the forerunner will have to be adjusted to account for the increase resistance as they drag through the layers. The value of $\bar{Q}$ Equation 3.12 can increase in according the additional resistance:

$$\frac{T_a}{2}(\theta_a^2 - \theta_0^2) = z\bar{Q} = N_{Cmult} 2bE_n N_c b\left(s_{uo} + \frac{kz}{2}\right) \quad (4.11)$$

$where;$
$N_{cmult} = mooring\ line\ resistance\ multiplier$
$T_a = padeye\ tension$
$\theta_o = mudline\ line\ angle$
$\theta_a = padeye\ line\ angle$
$z = padeye\ depth$
$\bar{Q} = average\ bearing\ resistance$
$b = forruner\ diameter$
$E_n = forrunner\ type\ multiplier\ (chain = 2.5, wire = 1)$
$N_c = chain\ bearing\ factor\ (10)$
$s_{uo} = mudline\ shear\ strength$
$k = shear\ strength\ gradient$

Above stiff layer: (4.12)

$$N_{cmult} = 1$$

In stiff layer: (4.13)

$$N_{cmult} = (s_{ur} - 1)\ \frac{s_{uo}(z - z_{S1}) + \frac{1}{2}k(z - z_{S1})^2}{s_{uo}z + \frac{1}{2}kz^2}$$

Below the stiff layer: (4.14)

$$N_{cmult} = (s_{ur} - 1)\ \frac{s_{uo}(z_{S2} - z_{S1}) + \frac{1}{2}k(z_{S2} - z_{S1})^2}{s_{uo}z + \frac{1}{2}kz^2}$$

$where;$
$N_{cmult} = mooring\ line\ resistance\ multiplier$
$s_{uo} = mudline\ shear\ strength$
$k = shear\ strength\ gradient$
$z = padeye\ depth$
$z_{s1} = depth\ to\ top\ of\ stiff\ layer$
$z_{s2} = depth\ to\ bottom\ of\ stiff\ layer$

The value of $d\theta_a$ can then be calculated using Equation 4.15, but it will not be the only factor creating rotation in the fluke. Still assuming the steady state condition, the fluke will rotate such that θ_a aligns with $\theta_{fs,}$ additional components of rotation will occur as θ_{fs} changes as it passes through the stiff layer.

$$d\theta_a = \frac{1}{\theta_a}\left(\frac{E_n N_c b N_{cmult}}{T_a} - \frac{k(\theta_a^2 - \theta_o^2)}{2s_{uo}}\right) ds \tag{4.15}$$

$where;$
$d\theta_a = change\ in\ padeye\ angle$
$E_n = forrunner\ type\ multiplier\ (chain = 2.5, wire = 1)$
$N_c = chain\ bearing\ factor\ (10)$
$b = forruner\ diameter$
$k = shear\ strength\ gradient$
$\theta_a = padeye\ line\ angle$
$\theta_o = mudline\ line\ angle$
$T_a = padeye\ resistance$
$s_{uo} = mudline\ shear\ strength$

As the fluke rotates it will seek to reorient itself to the updated θ_{fs} and θ_a.

$$\theta_f = \theta_{fs} - \theta_a \tag{4.16}$$

$where;$
$\theta_f = fluke\ angle$
$\theta_{fs} = fluke\ shank\ angle$
$\theta_a = padeye\ line\ angle$

4.4 Capacity Calculations

With the adjustments to the equivalent geometry to the anchor, the yield surface, and mooring line equations the capacity in layered soils is then calculated in the same fashion as in Section 4.4 now using the enhanced maximum bearing factors.

$$f = \left(\frac{sin(\theta_{fs})N_e}{N_{ne\,max}}\right)^q + \left(\frac{cos(\theta_{fs})N_e}{N_{te\,max}}\right)^{n/p} - 1 = 0 \quad (4.17)$$

$where;$
$f = equation\ of\ the\ yield\ locus$
$\theta_{fs} = fluke\ shank\ angle$
$N_e = effective\ bearing\ factor$
$N_{tmax}, N_{nmax} = maximum\ bearing\ factors$
$q, n, p = dimensionless\ coefficients$

The padeye tension is then:

$$T_a = N_e A_{fe} s_u \quad (4.18)$$

$where;$
$T_a = padeye\ capacity$
$A_{fe} = enhanced\ fluke\ area$
$N_e = effective\ bearing\ factor$
$s_u = undrained\ shear\ strength\ at\ the\ padeye$

4.5 Model Algorithm

The layered model relies on the same kinematic model as the base model utilizing incremental advance of the anchor, ds, parallel to the bottom of the fluke. Great care must be taken in the selection of ds to avoid advancing the anchor at too large of increments overstep the interface behavior as the anchor enters the stiff layer.

With the modification to the governing equations the steps now become:

1. Assume initial depth, z, at of the anchor at which it sets in
2. Check for embedment in stiff layer, and perform area transformations
3. Calculate equivalent geometry, y_{na}, L_{fe}, and W_{fe}, using Equation 4.2 - 4.4
4. Calculate θ_{fs} using Equation 4.5

5. Update the shape of the yield locus through Equation 4.6-4.7
6. Calculate N_e using Equation 4.17 and T_a using Equation 4.18
7. Calculate the θ_a using Equation 4.11 and $\theta_{f,}$, using Equation 4.16
8. Calculate R_{nt} using Equation 4.10
9. Calculate dz, and dx using Equation 3.6 & 3.7
10. Calculate T_o using Equation 3.15
11. Update x, z, and θ_f ($\theta_{f=} \theta_{f(i-1)}+ d\theta_a$)
12. Repeat steps 2-12 until θ_f approaches zero

Due to the lack of field and laboratory data for the installation of the DEA this model cannot be verified against actual measurement. The model however can be compared to general observations of the anchor such as tripping along soil interfaces.

4.6 Typical Model Behavior

Using the same soil and anchor properties as outlined for the base model in Section 3.5 the inputs were varied to allow the inclusion of a stiff layer. Behavior was observed through a range of simulation to show how the model captures the behavior of DEA through layered soils. Analyses were run for soft layer overlying a semi-infinite stiff with increasing s_{ur}, and for discrete layers varying thickness, s_{ur}, and depth.

The examples are specifically targeted to capture problematic behavior of DEA in layered soils including, tripping along boundaries, reaching capacity without penetrating stiff layers, and the failure to penetrate a layer due to shallow fluke angle.

4.6.1 Semi-Infinite Stiff Layer

For a semi-infinite stiff layer at a depth of 10m the s_{ur} was varied over a range of s_{ur}. The results are shown in Figure 29 - Figure 31. Three distinct behaviors can be seen; penetration, plowing, and tripping.

At lower s_{ur} values (1 to 3) the anchor achieves penetration into the stiff layer. As expected anchor penetration and capacity increases due to the increased bearing resistance in the stiffer soil. As the value of s_{ur} continues to increase the anchors begin to have difficulty embedding into the layer. Increases in s_{ur} begin to results in decreased embedment and capacity. In the case of $s_{ur} = 5$, the anchor fails to penetrate the layer through the layer and instead plows horizontally along the layer at a constant configuration with no changes in capacity or θ_f. If the stiffness of the layer is further increased as in the case of $s_{ur} = 8$ & 12 the anchor fails into the layer and instead trips along the interface embedding until the R_{nt} becomes > 1 and the anchor begins to pull out, at which the value of R_{nt} becomes < 1 and embedment continues, with the process repeating itself.

The model simulates this behavior through the enhanced geometry of the fluke and the distortion of the yield locus as the anchor embed in the layer. The area transformation results in a forward shift in y_{na} which increases the $\theta_{fs,}$ and shifts the location on the yield surface closer to the normal loading axis. In addition during partial embedment N_{temax} initially increases at a rate higher than N_{nemax} resulting an outward shift along the tangential loading axis. This movement along the yield surface and the distortion of the yield surface result in a norm that has a larger component of strain in the

normal direction to the anchor. This behavior can be visualized by plotting the yield locus for both the partial embedment and after pullout as seen in Figure 32. In this figure the configuration is initially at point a) before entering the layer with large components of the norm and therefore motion in the tangential direction, then as the anchor begins to embed into the layer the location on the yield surface shifts to point b) which has a significantly larger component of the norm and therefore motion in the direction normal to the fluke. On the plots of fluke angle represent a theoretical range of values as while tripping along the layer.

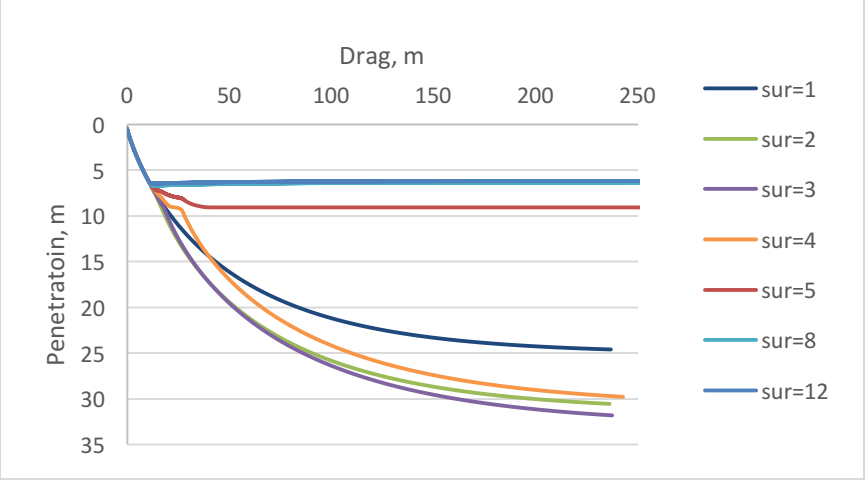

Figure 29: Trajectory Semi-Infinite Layer

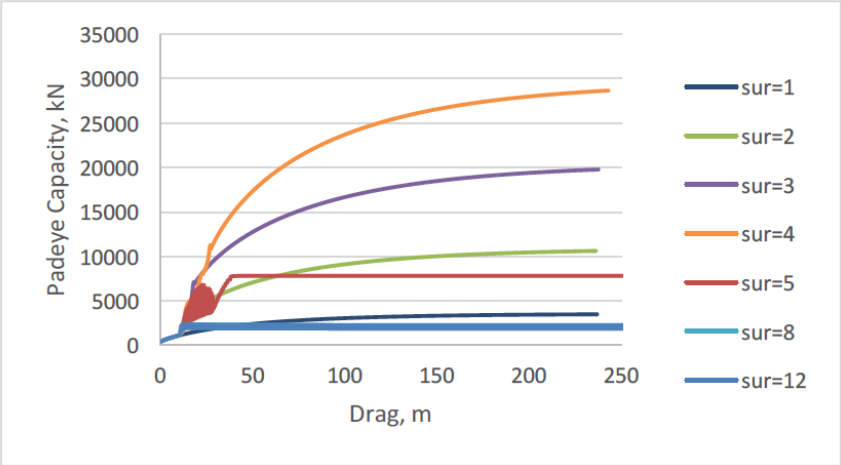

Figure 30: Capacity Semi-Infinite Layer

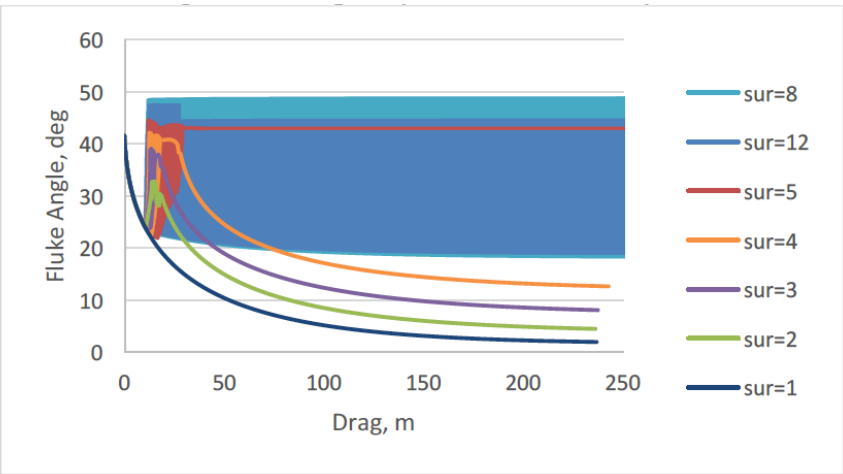

Figure 31: Fluke Angle Semi-Infinite Layer

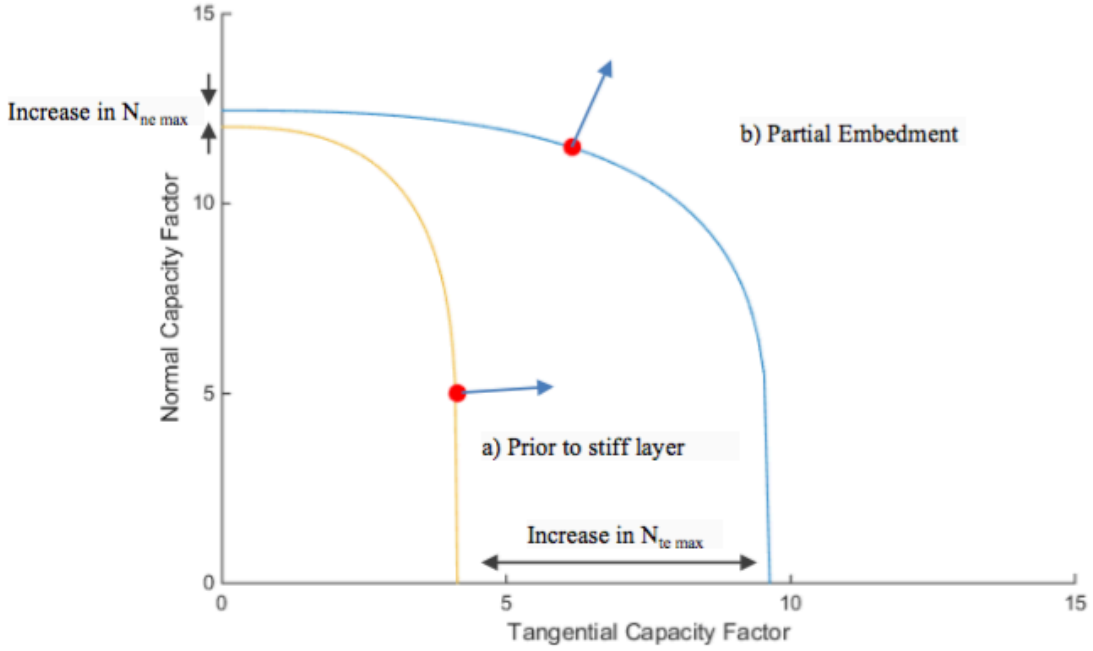

Figure 1: Yield Locus Evolution (s_{ur}=12)

4.6.2 Discreet Layer Varying s_{ur}

For a discreet layer at depth of 10 m, with a thickness of 1 m s_{ur} was varied over a range values. The results are shown in Figure 33 - Figure 35.

In the cases where the anchor penetrates the stiff layer ($s_{ur} < 4$) the trajectory and capacity return to values similar the case of no layer. While the anchor penetrates the stiff layer a significant increase in capacity is developed. This represents a situation where an anchor could partially embed into the stiff layer and achieve capacity without achieving adequate penetration. As these analyses are displacement controlled it can be seen that with increased load the anchor can break through the layer and then continue to

embed into the softer soil below. In field installation this may not be the case as this load may exceed the capacity of the AHW. In addition to increased sensitivity to out of plane loading this may also present a significant risk to the design of anchor if unexpected loads exceed the peak resistance created by the stiff layer and penetrate though the layer resulting in a rapid drop in capacity and significant drag. In the case of very stiff layers (s_{ur}>8) the anchor again show the tripping behavior described in Section 4.6.1.

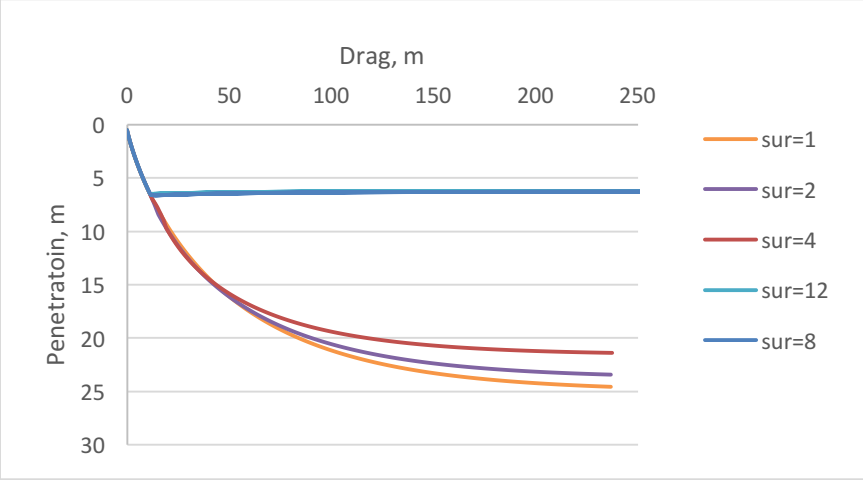

Figure 33: Trajectory Discrete Layer Varying s_{ur}

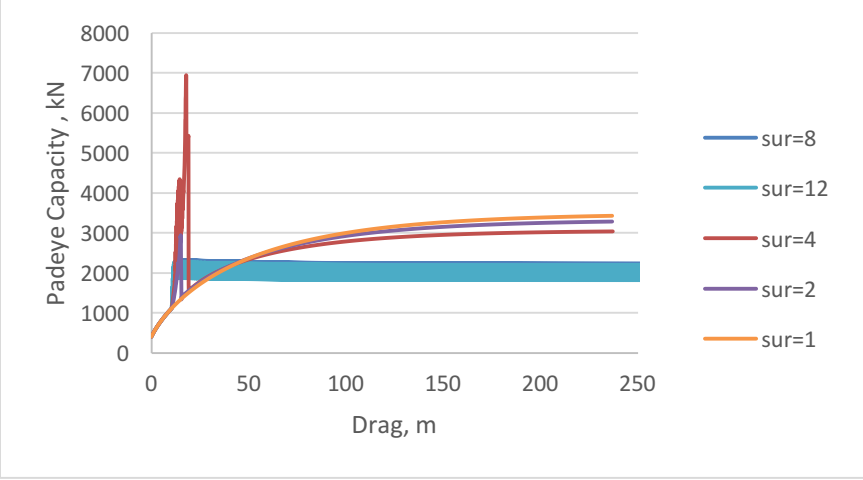

Figure 34: Capacity Discrete Layer Varying s_{ur}

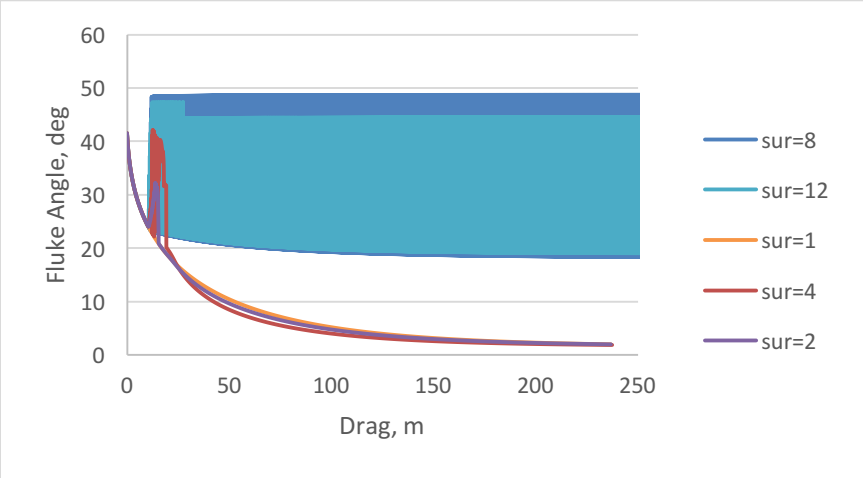

Figure 35: Fluke Angle Discrete Layer Varying s_{ur}

4.6.3 Discreet Layer Varying Depth

For a discreet layer with a thickness of 2 m s_{ur}=4 the depth of the stiff layer was evaluated for z_l=5m, 10m, and 15m and compared to the behavior without the stiff layer. The results are shown in Figure 36 - Figure 38.

At shallow depths the anchor was able to penetrate through the stiff layer. Once layer reached a depth beyond 15m it was no longer to penetrate through the layer, but did embed in the layer resulting in increased capacity. The failure to penetrate deeper layers may also be attributed to the use of a shear strength gradient and an s_{ur} which results in stronger layers at deeper depths.

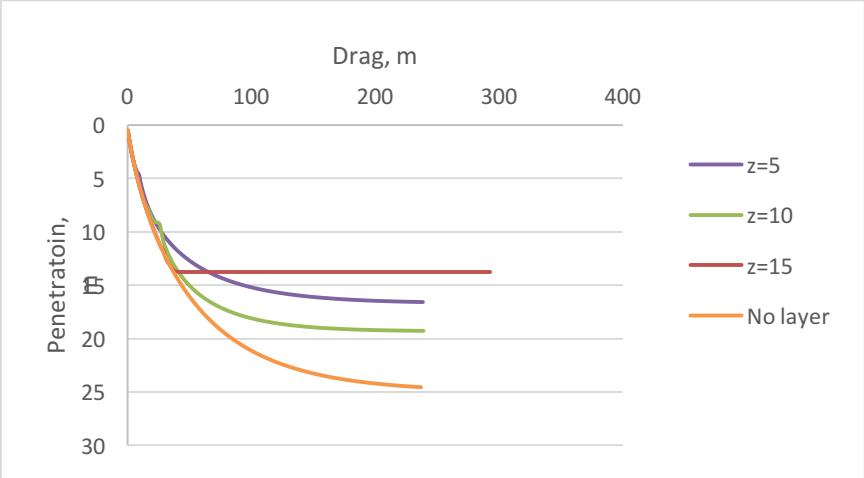

Figure 36: Trajectory Discrete Layer Varying Depth

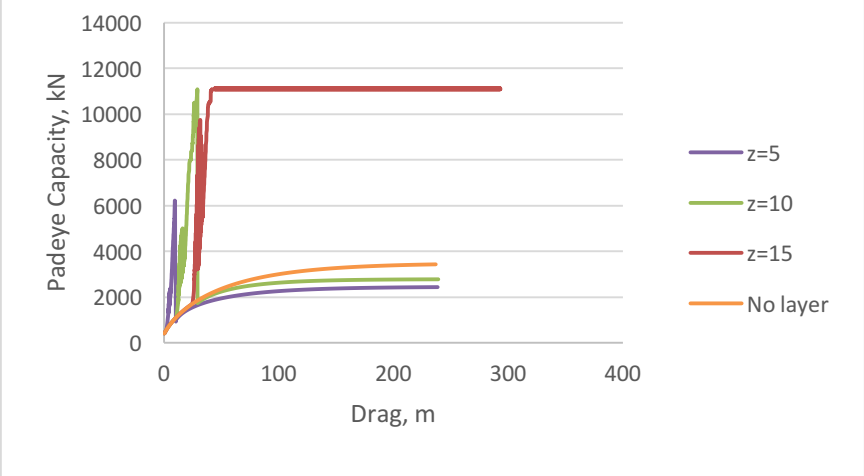

Figure 37: Capacity Discrete Layer Varying Depth

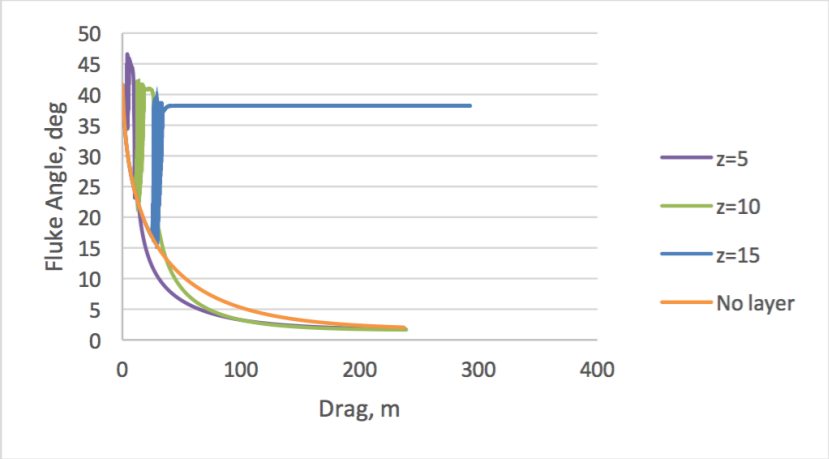

Figure 38: Fluke Angle Discrete Layer Varying Depth

5. SUMMARY AND CONCLUSIONS

5.1 Summary

While drag embedment anchors (DEA) have installed widely around the world, uncertainties in the prediction of their capacities, and trajectories during installation has presented a significant challenge to designers. Design charts widely used in industry for the design of DEAs rely heavily on empirical correlations and provide inadequate information for detailed designs. In order to reduce the level of empiricism and rely on geotechnical principles a number of limit equilibrium and plastic limit analyses have been proposed.

The models proposed here provide a simplified plastic limit analysis framework for the analysis of the trajectory and capacity of drag embedment anchors in cohesive soils. In plastic limit analyses anchors are incrementally advanced parallel to the fluke and a yield surface is used to evaluate the forces acting on the anchor. Assuming the displacements are the result of purely plastic strains and associated flow, the relative components of the displacement can be calculated using the norm of the yield surface. A simplified analysis assumes a steady state condition where the padeye load aligns with the neutral axis of the anchor. This steady state has two effects on the anchor. First to maintain this configuration angle the rotation of the fluke must be equal to the rotation of the padeye and therefore can be described by the evolution of the padeye load angle as it embed into the soil. Second since the load acts through the neutral axis the anchor the analyses results in a condition of zero moment and the analyses can be reduced to an interaction of normal and tangential forces acting on the anchor.

The presence of layered soils present an added level of complexity and a significant challenge to the design of DEA. During installation they can prevent anchors from achieving the desired embedment, and in some cases prevent the anchor from reaching the desired capacity due to it tripping along the interface between layers. The second model proposed here expands the model presented for uniform soils to allow for the inclusion of stiff cohesive layers of soil. Stiff layers are analyzed by transforming the region of the anchor in the layer proportionately to the stiffness ratio of the layer. This results in a continually changing equivalent geometry of the anchor, and distorts the shape of the yield surface as the anchor embeds through the layer. As no known publicly non-proprietary data exists for the installation of DEA in layered soil the model could not be validate. The models capability to capture known behavior was analyzed by simulations through a range of stiff soil conditions.

5.2 Conclusions

The following conclusions were made from the proposed models:

1. The UHC calculated using the base model match well with published design chart. Simulations for chain and wire forerunners bound the values presented in the design charts, with chains experience lower capacity and wires experiencing high capacity.
2. The result of the model compare well to field installations when an appropriate set-in drag and penetration is selected. Prior to the anchor setting in the anchor does not behave in a steady state condition and as such the model cannot capture the initial behavior.

3. The layered model was able to capture the behavior of anchor embedding into a stiff layer and then reaching capacity without penetrating the layer. In this case the anchor partially embeds and the capacity increases reaches the desired load. This can present a hazardous condition where under larger unexpected loads the anchor can punch through the stiff layer resulting in a loss of capacity and significant drag
4. In the presence of very stiff layers the model was able to capture the behavior of the anchor tripping along the interface. As the anchor embeds into the stiff layer the distortion of the yield surface and shift in θ_{fs} angle result in a increased component of displacement normal to the fluke, which can exceed the tangential displacement resulting in pullout. After partially extracting itself from the stiff layers the anchor then begins to re-embed into the layer and the process repeats.

5.3 Recommendations for Future Research

Recommendations for future research include:

1. Further validation of the base against installation data for the most current anchor designs
2. Validation of the layered soil model. This would require the development of scale testing, or centrifuge testing procedures as well as carrying out and interpreting the results
3. Development of anchor specific yield loci based on finite element studies to provide a more rigorous framework for predicting anchor kinematic behavior.

REFERENCES

Aubeny, C. Kim, B. and Murff, J. (2005). "Proposed Upper Bound Analysis for Drag Embedment Anchors in Soft Play." *Proc. Int. Symp. on Frontiers in Offshore Geotechnics*, Perth, Australia, 179-187.

Aubeny, C. Kim, B. and Murff, J. (2008). "Prediction of Anchor Trajectory During Drag Embedment in Soft Clay." *International Journal of Offshore and Polar Engineering*, Vol 18, 314-319.

Aubeny, C. and Chi, C. (2010). "Mechanics of Drag Embedment Anchors in a Soft Seabed." *Journal of Geotechnical and Geoenvironmental Engineering*, Vol 136, 57-68.

Aubeny, C. and Chi, C. (2014). "Analytical Model for Vertically Loaded: Anchor Performance." *Journal of Geotechnical and Geoenvironmental Engineering*, Vol 140, 14-24.

Bruce Anchors (n.d). "Bruce FFTS Mk 4 Anchor Datasheet", Bruce Anchors. Cronkbourne, Isle of Man.

Dahlberg, R. (1998) "Design Procedures for Deepwater Anchors in Clay." *Proc. 30th Offshore Technology Conference*, OTC 8837: Houston, TX, 560-560.

FMC Technologies (n.d). "Anadarko Independence Hub Data Sheet", FMC Technologies, http://www.fmctechnologies.com/en/SubseaSystems/GlobalProjects/North America/US/AnadarkoIndHub.aspx

Kim, B (2005). "Upper Bound Analysis for Drag Anchors in Soft Clay." PhD Dissertation, Texas A&M University, College Station, Texas.

Lelievre, B. and Tabatabaee J. (1981). "The Performance of Marine Anchors with Planar Flukes in Sand." *Canadian Geotechnical Journal*, Vol. 18, 520-537.

NAVFAC (2012). *Handbook for Marine Geotechnical Engineering*, Naval Facilities Engineering Command. Port Hueneme, California, SP-2209-OCN

NCEL (1987). "Drag Embedment Anchors for Navy Moorings", Naval Civil Engineering Laboratory. Port Hueneme, California, 86-08R

Murff, J. (1994). "Limit Analysis of Multi-Footing Foundation Systems" *In Proceedings of the 8th International Conference on Computer Methods and Advances in Geomechanics*. Morgantown, West Virginia, 223-244.

Murff, J. Randolph, M. Elkhatib, S. Kolk, H. Ruinen, R. Strom, P. and Thorne, C. (2005). "Vertically Loaded Plate Anchors for Deepwater Applications." *Proc. Int. Symp. on Frontiers in Offshore Geotechnics*, IS-FOG05, Perth, Australia, 31-48.

Neubecker, S.R. and Randolph, M.F. (1996a). "The Performance of Embedded Anchor Chains Systems and Consequences for Anchor Design." *Proc. 28th Offshore Technology Conference,* OTC 7712, Houston, Texas.

Neubecker, S.R. and Randolph, M.F. (1996b). "The Kinematic Behavior of Drag Anchors in Sand." *Canadian Geotechnical Journal*. Vol 33, 584-594.

Neubecker, S.R. and Randolph, M.F. (1996c). "The Static Equilibrium of Drag Anchors in Sand." *Canadian Geotechnical Journal*. Vol 33, 574-583.

O'Neill, M.P. (2000). "The Behavior of Drag Anchors in Layered Soils." PhD Dissertation, University of Western Australia, Perth, Australia.

O'Neill, M. Bransby, M. and Randolph, M. (2003) "Drag Anchor Fluke-Soil Interaction in Clay." *Canadian Geotechnical Journal*. Vol 40, 78-94.

Stewart, W.P. (1992) "Drag Embedment Anchor Performance Prediction in Soft Soils." *Proc. 24th Offshore Technology Conference,* OTC 6970, Houston, Texas.

Thorne, C. P. (1998). "Penetration and Load Capacity of Marine Drag Anchors in Soft Clay." *Journal of Geotechnical and Geoenvironmental Engineering*, Vol 124, 945-953.

Yang, M., Murff, J. and Aubeny, C. (2008). "Out of Plane Loading of Plate Anchors, Analytical Modeling, Phase II Report." Offshore Technology Research Center (OTRC), Texas A&M University, College Station, Texas.

Vryhof (2010). *Anchor Manual 2010 The Guide to Anchoring*, Vryhof Anchors. Capelle a/d Yssel, The Netherlands.